Distinct Mechanisms Underlie Regeneration of Mechanosensory Hair Cells in Zebrafish

Eric D. Thomas

A dissertation

submitted in partial fulfillment of the

requirements for the degree of

Doctor of Philosophy

University of Washington

2018

Reading Committee:

David Raible, Chair

Cecilia Moens

Thomas Reh

Program Authorized to Offer Degree:

Neuroscience

University of Washington

Abstract

Distinct Mechanisms Underlie Regeneration of Mechanosensory Hair Cells in Zebrafish

Eric D. Thomas

Chair of the Supervisory Committee:
Professor David Raible
Department of Biological Structure

The mechanosensory hair cells of the inner ear mediate hearing and balance. Widespread loss of these hair cells results in severe hearing and balance deficits. Humans and other mammals are unable to regrow lost hair cells, but there are a number of other organisms, such as fish, frogs, and birds, that can. A more thorough understanding of how this hair cell regeneration occurs, at the genetic, molecular, and cellular levels, could one day allow us to target those same processes in humans and induce endogenous hair cell regeneration as a therapy for hearing and balance disorders. The zebrafish is one such organism that serves as an excellent model for hair cell regeneration. Zebrafish not only have an inner ear, but also a sensory system called the lateral line, which is comprised of clusters of hair cells arranged along the surface of the body. Lateral line hair cells are analogous to inner ear hair cells, but mediate the fish's response to changing water flow. Previous studies have demonstrated that lateral line hair cells regenerate rapidly and completely following hair cell death, and that the surrounding support cells serve as progenitors for new hair cells. However, little is known about how progenitor function in the lateral line is regulated, and the work presented in this thesis seeks to rectify that.

In Chapter 1 I provide an introduction to hair cell regeneration, with a particular focus on hair cell regeneration in the zebrafish lateral line and the inner ear. In Chapter 2, I identify genetically-distinct populations of lateral line support cells and demonstrate that they differ in their capacities to serve as hair cell progenitors. Furthermore, I show that these progenitor populations are independently regulated and that they also serve to maintain the progenitor pool within the lateral line. In Chapter 3, I develop tools to study regeneration of zebrafish inner ear hair cells and demonstrate that regeneration in the cristae occurs via transdifferentiation. Finally, in Chapter 4 I summarize my work and outline future experiments that will further elucidate our understanding of the mechanisms underlying hair cell regeneration.

TABLE OF CONTENTS

LIST OF FIGURES

ACKNOWLEDGEMENTS

It has indeed been a long and winding road. I'd be lying if I claimed that my seven-and-a-quarter years in graduate school weren't fraught with hardship; that would be an understatement. Yet, in spite of all the uphill battles, I have accomplished something I can truly be proud of. And I wouldn't have gotten to this point without the aid of a lot of wonderful people, whom I'd like to acknowledge now.

I must begin with my advisor, Dave Raible. In addition to being a fantastic scientist, Dave also takes great care to ensure the success of his students. We may not have been on the same wavelength during my early years in the lab, but I never doubted that Dave had my best interests at heart, and he refused to give up on me during my darkest, bleakest moments. His mentorship has also been instrumental in developing my scientific communication skills. I fancied myself a good writer coming out of undergrad, having studied Classics and all, but his input, whether during lab meetings, practice talks, or DBTG-related events, allowed me to improve my writing and presentation skills beyond what I thought was possible. Thank you for everything Dave! I look forward to continue on in the Seattle developmental biology community as a colleague.

I cannot praise Dave without also praising the fantastic laboratory environment that he has built over the years. I have seen the Raible Lab expand and condense throughout my tenure, but it has always been an incredibly fun and supportive place to work. Filled with brilliant scientific minds, a collaborative atmosphere, and penchant for (sometimes) good wordplay, the lab and its people have always made me feel at home. I must particularly thank postdocs such as Robert Esterberg, Joy Sebe, and Dale Hailey, as well as my fellow grad students-in-fins Ivan Cruz, Sarah Pickett, and Maddy Hewitt for their constant care and support over the many years. I look forward to the work that will come out of the lab in the future.

I would also like to thank the members of my thesis committee – Cecilia Moens, Rachel Wong, Tom Reh, David Kimelman, and Jay Parrish – for their support and input towards my thesis project over the years. Their insight and guidance were essential for the completion of my project.

I wouldn't have been able to survive this long were it not for the constant support of the many amazing friends I have made throughout my graduate career. From kickball and fantasy football to Game of Thrones trivia, board game nights, and beerfests, my friends have always been there for me, whether it was in celebration or in consolation. I would like to especially thank Sarah Pickett, Florie D'Orazi, Jay Chakkera, Amanda Wunsch, Max Turner, Brian Schmidt, Leah Bakst, Wambura Fobbs, Aiva Ievins, Matt Brodsky, Steph Seeman, Sweta Agrawal, Jacob Nettleton, Clare Gamlin, and Leah VandenBosch for their continued support over the years. I love you all.

I must offer a truly special thanks to my parents, Steve Thomas and Karyn Gotthardt. Among other things, they instilled in me an unparalleled work ethic and the drive to never give up, both of which were essential to my success in graduate school. My mother was tragically diagnosed with frontotemporal dementia during my fourth year in graduate school, which certainly took its toll on my psyche. However, my father took the entire burden of her care upon his shoulders, so that I could advance my research with as few hang-ups as possible. Thank you, Dad, for everything you've done; your struggle gave me strength when I needed it most. And Mom, if you are able to understand these words, I want to thank you for everything you've done for me, and I hope I've made you proud. I love you.

Finally, I'd like to thank my wonderful partner Maddy. She may have joined my party late in the quest, but she has been a constant source of joy and support over the last year, and has challenged me to become a better person, both scientifically and personally. I am excited to see where her immense scientific talents will take her in the future.

ET
Seattle, 2018

CHAPTER 1

INTRODUCTION

Hair cells are mechanosensory receptors located within the inner ear that are responsible for mediating our senses of hearing and balance. Widespread loss of these cells, whether due to developmental disorders, aging, or exposure to excessive noise or ototoxic compounds, results in severe hearing and balance deficits. Unfortunately for us, these deficits are irreversible in humans and result in a number of common disorders. For instance, roughly 25 million Americans suffer from some form of hearing loss, and 69 million Americans experience vestibular disfunction such as vertigo (Agrawal, Carey, Della Santina, Schubert, & Minor, 2009; Goman & Lin, 2016). However, there are a number of other organisms, such as birds and fish, that are capable of regenerating their hair cells after damage and thus restoring auditory and vestibular function. If we can understand the precise mechanisms underlying hair cell regeneration in these organisms, and how they differ from mammals, then we could potentially be able to, one day, induce endogenous hair cell regeneration in humans as a treatment for these hearing and balance disorders.

The goal of this thesis work is to elucidate the mechanisms underlying hair cell regeneration in zebrafish, and in particular the cells that serve as hair cell progenitors. In the following chapter, I provide background on the differences in regenerative capacity between organisms, with a specific focus on the zebrafish lateral line system. In Chapter 2, I will describe my work examining functionally distinct progenitor populations in the zebrafish lateral line and how they mediate not only hair cell regeneration, but also the replacement of other progenitor cells. In Chapter 3, I will describe some recent preliminary work examining hair cell

regeneration in the zebrafish inner ear, and in Chapter 4 I will summarize my findings and provide some future directions.

1.1 Hair Cell Regeneration in Birds and Mammals

Birds (in particular the chicken inner ear) have long been an excellent model for hair cell regeneration. Early studies showed that hair cells in the basilar papilla (the avian auditory organ) were capable of regenerating after noise- or aminoglycoside-induced damage (Cotanche, 1987; R. M. Cruz, Lambert, & Rubel, 1987). These regenerated hair cells are derived from the surrounding support cells, which serve has hair cell progenitors through two distinct mechanisms: direct transdifferentiation, or the phenotypic conversion from one cell type to another without cell division, and mitotic division. Support cell transdifferentiation accounts for the earliest regenerated hair cells, with later addition occurring via proliferation (Corwin & Cotanche, 1988; David W. Roberson, Alosi, & Cotanche, 2004). Preventing proliferation with mitotic inhibitors reduces the number of regenerated hair cells, but does not affect early transdifferentiation (Adler & Raphael, 1996; Shang, Cafaro, Nehmer, & Stone, 2010). Rather importantly, the regeneration of hair cells leads to recovery of auditory and vestibular function (Carey, Fuchs, & Rubel, 1996; Girod, Tucci, & Rubel, 1991; Goode, Carey, Fuchs, & Rubel, 1999; Tucci & Rubel, 1990).

Unlike birds, mammals have shown very little capacity for regeneration following hair cell damage. However, early studies showed distinct differences between auditory and vestibular epithelia: while auditory support cells remained quiescent after hair cell damage, vestibular support cells proliferated and were able to generate some cells that had some hair cell-like characteristics *in vitro* (Forge, Li, & Nevill, 1998; D W Roberson & Rubel, 1994; Sobkowicz, August, & Slapnick, 1997; Warchol, Lambert, Goldstein, Forge, & Corwin, 1993). This inability

to form functional hair cells in spite of support cell proliferation was confirmed in later *in vivo* studies (Li & Forge, 1997; Oesterle, Cunningham, Westrum, & Rubel, 2003; Ogata, Slepecky, & Takahashi, 1999). A more recent study has demonstrated that support cells are capable of transdifferentiating into hair cells following genetic ablation in the utricle, although the number of regenerated hair cells remained fairly low (Bucks et al., 2017).

The reasons underlying mammals' general inability to regenerate their hair cells has remained a mystery. It was hypothesized that the lack of ongoing proliferation in the mature auditory and vestibular epithelia prevented any future progenitor activity. Hair cell genesis and support cell proliferation are high during embryogenesis, but cease about two weeks after birth (J. C. Burns, On, Baker, Collado, & Corwin, 2012; Sans & Chat, 1982; White, Doetzlhofer, Lee, Groves, & Segil, 2006). In contrast, new hair cells are generated in the avian vestibular epithelium throughout the lifespan of the animal (D. F. Roberson, Weisleder, Bohrer, & Rubel, 1992). However, hair cells are not continuously generated in the chick basilar papilla, and yet they are still able to regenerate following damage (Jørgensen & Mathiesen, 1988). Thus, lack of ongoing hair cell generation cannot alone account for the lack of regenerative capacity in the mammalian inner ear. An alternate explanation could be the differences in the cytoskeletal architecture of support cells. Support cells in birds and neonatal mice have thin bands of filamentous actin (F-actin) lining their junctions with hair cells and other support cells, as well as low levels of E-cadherin. However, these size of these F-actin bands, as well as the levels of E-cadherin, increase dramatically as mice age, which correlates with a decline in support cell proliferation and hair cell generation (J. Burns et al., 2008; J. C. Burns, Collado, Oliver, & Corwin, 2013; J. C. Burns & Corwin, 2014; Collado et al., 2011; Guerra, de Lara, Malizia, & Díaz, 2009). Therefore, these differences in cytoskeletal properties could prevent mammalian

support cells from serving as hair cell progenitors in response to damage. Whether this is true remains to be seen.

A number of studies have attempted to induce hair cell regeneration in mammals by targeting the mechanisms involved in hair cell development. One such mechanism is Notch-mediated lateral inhibition, which regulates whether cells develop as hair cells or support cells. Activation of the Notch receptor induces expression of the transcription factor Hes5, which in turn represses Atoh1, a bHLH transcription factor that is required for hair cell differentiation (Bermingham et al., 1999). In the absence of Notch signaling, cells will retain their expression of Atoh1 and thus differentiate into hair cells. However, cells expressing Notch ligands will prevent their neighbors from expressing Atoh1, thus causing them to differentiate into support cells. Notch signaling thus regulates the development of the auditory and vestibular epithelia by regulating the spatial expression pattern of Atoh1 (Daudet & Lewis, 2005). Overexpression of Notch signaling represses hair cell differentiation (Daudet & Lewis, 2005), whereas inhibition of Notch ligands results in the generation of supernumerary hair cells (Kiernan, Xu, & Gridley, 2006; Yamamoto et al., 2006). In mammals, Notch signaling is active during embryonic development, but declines during the early postnatal weeks and is not present in the mature cochlea, although it is maintained at low levels in vestibular support cells, particularly in the cristae (Hartman et al., 2009; Slowik & Bermingham-McDonogh, 2013).

Notch signaling plays a similar role during hair cell regeneration: Notch inhibition (with the γ-secretase inhibitor DAPT) in the regenerating chick basilar papilla also results in the overproduction of new hair cells, while Notch overexpression prevents the formation of new hair cells (Daudet et al., 2009). However, Notch inhibition only results in supernumerary hair cell regeneration following hair cell damage; it is not sufficient to increase hair cell number in the

absence of damage. Since Notch signaling is relatively absent in the mature mammalian inner ear, it is unlikely that inhibiting it would increase hair cell numbers after damage. In fact, Notch signaling does not increase following hair cell damage (Hartman et al., 2009). Interestingly however, Notch inhibition following utricular hair cell death results in an increase in cells expressing Atoh1 *in vitro*, although these cells do not form fully mature hair cells (Lin et al., 2011). Furthermore, DAPT treatment of cultured cristae results in the generation of new hair cells via transdifferentiation (Slowik & Bermingham-McDonogh, 2013). In addition, treatment of noise-damaged cochleae with the more potent γ-secretase inhibitor LY411575 induces the formation of new hair cells, both *in vitro* and *in vivo*, and also results in a partial restoration of auditory function (Mizutari et al., 2013). Thus, it is possible that Notch signaling could still play a role in the damaged mammalian inner ear, and its future modulation could provide an attractive strategy for inducing hair cell regeneration in the mammalian inner ear.

1.2 Hair Cell Regeneration in the Zebrafish

In addition to birds, there are a number of other non-mammalian vertebrates, such as amphibians and fish, that are also capable of hair cell regeneration. In particular, the lateral line system of the zebrafish (*Danio rerio*) has become an incredibly powerful tool for studying the process in recent years. The lateral line is a sensory system comprised of clusters of cells called neuromasts arranged in a stereotypic fashion along the surface of the body (Fig 1.1). Each of these neuromasts is comprised of a cluster of mechanosensory hair cells surrounded and intercalated by support cells. Lateral line hair cells are structurally and functionally analogous to the hair cells of the inner ear, but they encode information about surrounding water fluctuation as opposed to sound, aiding in behaviors such as schooling, prey detection, and predator avoidance.

These hair cells are innervated by peripheral nerves, which transmit information to the hindbrain for further processing. Because these neuromasts are located on the surface of the body, they are easily accessible for visualization and manipulation without the need for dissection. Coupled with the transparency of zebrafish larvae and genetic tractability of the zebrafish as a whole, the lateral line is a fantastic model in which to study the genetic, molecular, and cellular mechanisms underlying hair cell development, function, and regeneration.

Lateral line hair cells are susceptible to a number of different chemical agents. Treatment with aminoglycoside antibiotics (Harris et al., 2003; Williams & Holder, 2000), chemotherapeutics (Ou, Raible, & Rubel, 2007), or heavy metals (Hernández, Moreno, Olivari, & Allende, 2006; Linbo, Stehr, Incardona, & Scholz, 2006) all result in hair cell death. However, new hair cells are generated following all of these treatments, generally returning to their pre-damaged numbers in about three days (Fig. 1.2) (Hernández, Olivari, Sarrazin, Sandoval, & Allende, 2007; Ma, Rubel, & Raible, 2008; Williams & Holder, 2000). Functional lateral line recovery accompanies this regeneration, as behaviors such as predator avoidance and rheotaxis (the ability to orient in opposing water flow) are reestablished as hair cells are regenerated (McHenry, Feitl, Strother, & Van Trump, 2009; Suli, Watson, Rubel, & Raible, 2012).

Unlike the avian inner ear, lateral line hair cell regeneration occurs predominantly via proliferation of surrounding support cells. Incubation in the thymidine analog BrdU for the first twenty-four hours after hair cell death labels the vast majority of regenerated hair cells (Ma et al., 2008; Romero-Carvajal et al., 2015; Wibowo, Pinto-Teixeira, Satou, Higashijima, & López-Schier, 2011). One earlier study concluded that some regeneration also occurred via transdifferentiation, since hair cell regeneration following copper-induced damage yielded a substantial number of BrdU-negative hair cells (Hernández et al., 2007). However, the copper

treatments in this study were administered at three days post fertilization (dpf), an age where neuromasts have not fully matured. Thus, the BrdU-negative hair cells in this case could have reflected ongoing hair cell development, as well as a small number of post-mitotic support cells that were already in the process of differentiating into hair cells but were not susceptible to damage. To confirm this, later studies demonstrated that administering mitotic inhibitors following hair cell death prevented new hair cells from forming (Mackenzie & Raible, 2012; Wibowo et al., 2011). Furthermore, subsequent timelapse imaging studies showed that regenerated hair cells arose from symmetric division of support cells (López-Schier & Hudspeth, 2006; Mirkovic, Pylawka, & Hudspeth, 2012; Romero-Carvajal et al., 2015; Wibowo et al., 2011). Thus, while transdifferentiation cannot be completely dismissed, support cell proliferation is the predominant mechanism by which hair cell progenitors generate new hair cells.

Similar to birds and mammals, zebrafish lateral line hair cell development and regeneration are regulated by Notch signaling. Mutants in which Notch signaling is inhibited, such as the *mind bomb* mutant, develop excess hair cells at the expense of support cells (Haddon, Jiang, Smithers, & Lewis, 1998). Similarly, inhibition of Notch signaling results in about twice the usual number of regenerated hair cells following damage (Ma et al., 2008; Romero-Carvajal et al., 2015). However, unlike in the avian basilar papilla, Notch inhibition in the absence of hair cell damage does not stimulate excess hair cell formation. Thus, it would seem that Notch signaling does not maintain support cell quiescence during homeostasis, but rather serves to ensure the proper number of hair cells are formed during regeneration. However, I have personally seen, on multiple independent occasions, that Notch inhibition via LY411575 is sufficient to generate supernumerary hair cells in the absence of hair cell damage. This could be due to the fact that LY411575 is a more potent Notch inhibitor than DAPT. In fact, DAPT

treatment has previously be shown to be insufficient to completely inhibit Notch signaling (Matsuda & Chitnis, 2010). It could thus be the case that Notch inhibition is a sufficient signal to cause hair cell progenitors to generate new hair cells during homeostasis. More experiments are needed on this front.

The symmetric division of support cells to generate new hair cells raises an interesting question about the long-term regenerative capacity of lateral line neuromasts. If a progenitor divides to make two daughter hair cells, and isn't itself replaced, then the progenitor pool could be depleted over time as neuromasts accrue damage. However, recent studies have shown that adult zebrafish are capable of proper hair cell regeneration after multiple successive hair cell ablations (I. A. Cruz et al., 2015; Pinto-Teixeira et al., 2015), indicating that there must be a mechanism by which hair cell progenitors themselves are replenished. This raises an even larger question about lateral line support cells: are there functionally distinct progenitor populations? Are there distinct subsets of support cells that serve as hair cell progenitors and others that replenish those progenitors? Recent studies have shown that support cell proliferation is spatially restricted within the neuromast, with progenitors primarily residing in the dorsal and ventral regions of the neuromast (I. A. Cruz et al., 2015; Romero-Carvajal et al., 2015; Wibowo et al., 2011). Is there something special about support cells in these regions relative to other support cells? There has been recent evidence of genes that are asymmetrically expressed throughout the neuromast (Steiner, Kim, Cabot, & Hudspeth, 2014). Perhaps these asymmetrically-expressed genes could define distinct populations of support cells. This will be explored further in Chapter 2.

1.3 Hair Cell Regeneration in the Zebrafish Inner Ear

While the zebrafish lateral line has received a lot of attention in recent years, zebrafish also have an inner ear that is capable of regeneration. In larvae, the inner ear is comprised of three cristae, which mediate vestibular function, and the saccule and utricle, which mediate auditory and vestibular function (Nicolson, 2005). These organs develop rapidly and are fully functional around 5 dpf (Vanwalleghem, Heap, & Scott, 2017). An additional sensory epithelium, the lagena, develops during the juvenile stage (Bever & Fekete, 2002). There have not been many studies examining hair cell regeneration in the inner ear, likely because the lateral line is simply an easier system with which to work. The few studies that have been performed have come to different conclusions about the mechanism of regeneration. One study examined regeneration in the larval utricle following laser ablation. A substantial number of hair cells regenerated within 24 hours of damage, and incubation in BrdU revealed no BrdU-labeled hair cells. Lineage analysis indicated that new hair cells were derived from surrounding support cells (Millimaki, Sweet, & Riley, 2010).

Another study examined regeneration in the adult saccule. New hair cell bundles were observed following noise-induced damage, although the time course for regeneration was substantially longer than in larvae (about 14 days). Many BrdU-labeled cells were observed throughout the saccule a few days after damage, but these labels did not colocalize with hair cell markers since the authors only observed hair cell bundles and not cell bodies (Schuck & Smith, 2009). The authors concluded that proliferation mediated hair cell regeneration since this proliferation was followed by the appearance of immature hair cell bundles, but it is possible that transdifferentiation could also play a role. In Chapter 3, I will reexamine hair cell regeneration in the larval inner ear in order to provide some clarity on the mechanism of regeneration.

1.4 Figures

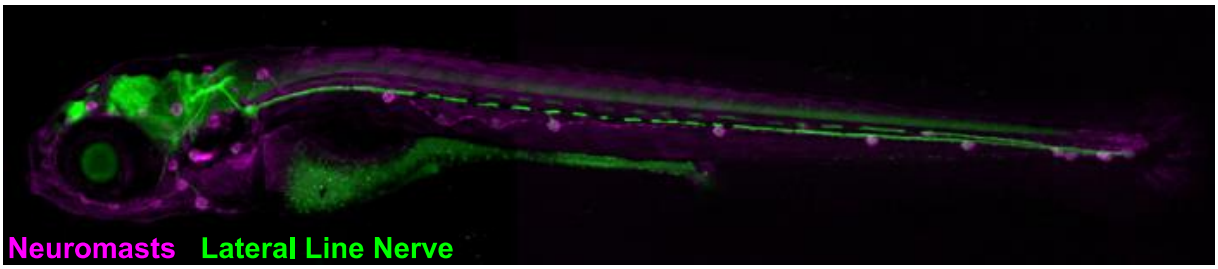

Figure 1.1 The zebrafish lateral line system. Maximum projection of a 5 dpf zebrafish larva. The head is located on the left. Individual neuromasts along the head and trunk are visualized in magenta. The nerves innervating the neuromasts on the trunk are shown in green. This figure was adapted with permission from Thomas et al. 2015.

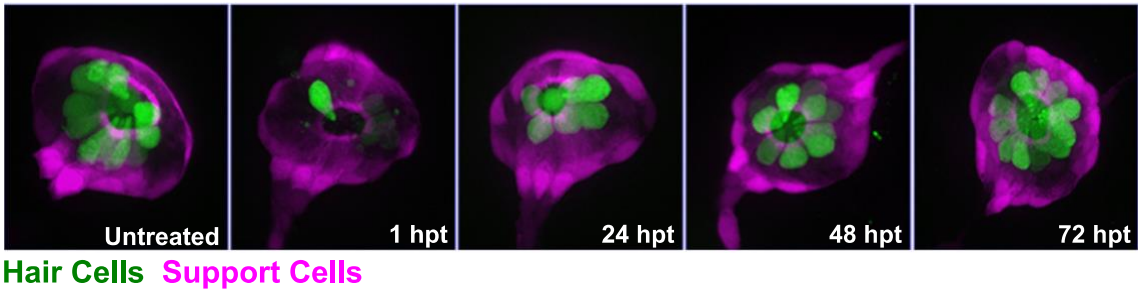

Figure 1.2 Lateral line hair cells regenerate following damage. Maximum projections of a neuromast prior to, 1, 24, 48, and 72 hours post treatment (hpt) with the ototoxic aminoglycoside antibiotic neomycin. Hair cells are shown in green and a subset of support cells are show in magenta. Treatment with neomycin kills almost all hair cells within an hour. However, new hairs cells are gradually added, reaching their pre-treatment numbers around 72 hpt. This figure was adapted with permission from Thomas et al. 2015.

CHAPTER 2

DISTINCT PROGENITOR POPULATIONS MEDIATE REGENERATION IN THE ZEBRAFISH LATERAL LINE

The contents of this chapter have been submitted for publication with the following authors: Eric D. Thomas and David W. Raible

2.1 Summary

Mechanosensory hair cells of the zebrafish lateral line regenerate rapidly following damage. These renewed hair cells arise from the proliferation of surrounding support cells, which undergo symmetric division to produce two hair cell daughters. Given the continued regenerative capacity of the lateral line, support cells presumably have the ability to replenish themselves. Utilizing novel transgenic lines, we identified support cell populations with distinct progenitor identities. These populations show differences in their ability to generate new hair cells during homeostasis and regeneration. Targeted ablation of support cells reduced the number of regenerated hair cells. Furthermore, progenitors regenerated after targeted support cell ablation in the absence of hair cell damage. We also determined that distinct support cell populations are independently regulated by Notch signaling. The existence of independent progenitor populations could provide flexibility for the continued generation of new hair cells under a variety of conditions throughout the life of the animal.

2.2 Introduction

The regenerative potential of a given tissue is dependent on the availability of progenitor cells that are able to functionally replace lost or damaged cells within that tissue. For instance, bulge cells in the hair follicle can repair the surrounding epidermis (Hsu, Li, & Fuchs, 2014; Rompolas & Greco, 2014), new intestinal epithelial cells arise from crypt cells (Santos, Lo, Mah,

& Kuo, 2018; Yousefi, Li, & Lengner, 2017), and horizontal and globose basal cells can regenerate cells in the olfactory epithelium (Choi & Goldstein, 2018; Schwob et al., 2017). Depletion of these progenitors can severely diminish the regenerative capacity of the tissue, and tissues that lack a progenitor pool altogether are unable to regenerate. To gain further insight into how different tissues regenerate, a greater understanding of the mechanisms that define and regulate progenitor function are needed.

The zebrafish lateral line system has long been recognized as an excellent model for studying regeneration. The sensory organ of the lateral line, the neuromast, is comprised of mechanosensory hair cells organized on the surface of the head and body (Thomas et al., 2015). Lateral line hair cells regenerate rapidly following damage, with the system returning to quiescence after regeneration is complete (Harris et al. 2003; Hernandez et al., 2007; Ma et al., 2008). The surrounding nonsensory support cells serve as progenitors for new hair cells. This replenishment is proliferation-dependent and occurs symmetrically, with each progenitor dividing to give rise to two daughter hair cells (Wibowo et al. 2011; Mackenzie and Raible 2012; López-Schier and Hudspeth 2006; Romero-Carvajal et al. 2015). Three key observations of support cell behavior during regeneration suggest that different support cell populations may be differentially regulated in response to regeneration. First, the support cell proliferation that follows hair cell death occurs mainly in the dorsal and ventral compartments of the neuromast (Romero-Carvajal et al. 2015), indicating that progenitor identity is spatially regulated. The most peripheral support cells, often called mantle cells, do not proliferate in response to hair cell damage (Ma et al., 2008; Romero-Carvajal et al., 2015). Second, the regenerative capacity of the neuromast is not diminished over multiple regenerations (I. A. Cruz et al., 2015; Pinto-Teixeira et al., 2015), indicating that progenitor cells must also be replaced in addition to hair cells.

Finally, in addition to regeneration in response to acute damage, lateral line hair cells undergo turnover and replacement under homeostatic conditions (I. A. Cruz et al., 2015; Williams & Holder, 2000). However, it remains unknown whether there are distinct support cell populations within the neuromast (e.g. hair cell progenitors and those that replenish progenitors), as well as how progenitor populations are regulated.

In this study, we have used CRISPR to generate novel transgenic lines in which distinct, spatially segregated populations of support cells are labeled *in vivo*. Fate mapping studies using these lines show that these populations are functionally distinct with respect to their ability to contribute new hair cells during homeostasis and to generate hair cells after damage. We also show that targeted ablation of one of these populations significantly reduces hair cell regeneration. Other fate mapping studies show that these support cell populations can replenish each other in the absence of hair cell damage. Finally, we show that Notch signaling differentially regulates these populations. These results demonstrate that there are a number of distinct progenitor populations within lateral line neuromasts that are independently regulated, and offer a greater understanding of how regeneration occurs in the zebrafish lateral line.

2.3 Results

2.3.1 Hair Cell Progenitors are Replenished via Proliferation of Other Support Cells

Previous studies have shown that the majority of support cell proliferation occurs during the first twenty-four hours following hair cell death (Ma et al., 2008). We replicated this finding by administering a pulse of F-ara-EdU (EdU), which has been shown to be far less toxic than BrdU (Neef & Luedtke, 2011). The EdU pulse was administered for twenty-four hours following neomycin-induced hair cell ablation at 5 days post fertilization (5 dpf) and neuromasts were

imaged at seventy-two hours post treatment (72 hpt), the time at which regeneration is nearly complete (Fig. 2.1A). In neomycin-treated larvae, roughly 78% of regenerated hair cells were EdU-positive, compared to 6% in mock-treated larvae (Fig. 2.1B-C; $p < 0.0001$). We noticed that at the same timepoint that 28% of EdU-positive cells remained support cells (Fig. 1E, 1B arrowheads). We hypothesized that these cells may represent hair cell progenitors that had been replaced via proliferation. If so, then these EdU-positive cells should have the capacity to generate a new round of hair cells after subsequent damage. In order to test this, we subjected larvae to two rounds of hair cell ablation and regeneration. EdU was administered for 24h following the first ablation, and BrdU was administered for the same duration following the second ablation (Fig. 2.1F). We observed hair cells after the second regeneration that were both EdU- and BrdU-positive (Fig. 2.1G-J, arrowheads), indicating that support cells that divide after the first ablation can in fact serve as hair cell progenitors after subsequent damage. However, we also observed double-positive cells that remained support cells (Fig. 2.1K-N, arrowheads), as well as support cells that were only labeled by EdU (Fig. 2.1G-N, asterisks). These observations indicate that support cells that divided after the first round of damage do not always serve as hair cell progenitors (or even as progenitors at all). Altogether, these data provide evidence of proliferation-mediated replenishment of hair cell progenitors by support cells in the neuromast, but also suggest that new hair cells arise from a pool of progenitors that are not strictly defined by their proliferation history.

2.3.2 Different Progenitor Identities Among Distinct Support Cell Populations

We next sought to determine whether hair cell progenitors could be defined via gene expression. To this end, we employed CRISPR-mediated transgenesis (Kimura, Hisano,

Kawahara, & Higashijima, 2014; Ota et al., 2016) to target genes that label positionally-defined subsets of support cells *in vivo*. We targeted the expression of a nuclear-localized form of the protein Eos (nlsEos) to a variety of genetic loci, and identified three genes (*sfrp1a*, *tnfsf10l3*, and *sost*) which have markedly different expression patterns within support cells: *sfrp1a* is restricted to the most peripheral support cells (Peripheral cells; Fig. 2.2A); *tnfsf10l3* is more broadly expressed throughout the periphery but is enriched in anteroposterior support cells (AP cells; Fig. 2.2C); and *sost* is limited to the dorsal and ventral support cells (DV cells; Fig. 2.2E). We generated stable transgenic lines for all three loci: Tg[*sfrp1a*:nlsEos]^{w217}; Tg[*tnfsf10l3*:nlsEos]^{w218}; and Tg[*sost*:nlsEos]^{w215} (hereafter known as *sfrp1a*:nlsEos, *tnfsf10l3*:nlsEos, and *sost*:nlsEos, respectively). Eos is a photoconvertible protein that switches from green to red fluorescence (shown in magenta throughout this paper) after exposure to UV light (Wiedenmann et al., 2004). The converted protein is stable for months. Its nuclear localization presumably protects it from degradative elements in the cytoplasm, allowing for a more permanent label than a standard fluorescent reporter (I. A. Cruz et al., 2015; McMenamin et al., 2014). We could thus chase this label from support cell to hair cell if these cells serve as hair cell progenitors, as hair cells that derived from these support cells would have converted Eos in their nuclei. To ensure that these genes were not actually expressed in hair cells, we also generated GFP lines for each gene. We did not observe GFP labeling in hair cells in stable lines (Supplemental Fig. 2.13).

We first examined how these different support cell populations contributed to hair cell development and turnover under homeostatic conditions. All three nlsEos lines were crossed to a hair cell-specific transgenic line (Tg[Brn3c:GAP43-GFP]^{s356t} (Xiao et al., 2005), hereafter known as brn3c:GFP) in order to distinguish hair cell nuclei. Eos in support cells was

photoconverted at 5 dpf and larvae were fixed and immunostained for GFP either immediately or at 8 dpf. At 5 dpf, 19% of hair cells were labeled with Eos expressed by the Peripheral cell transgene, and this number remained the same by 8 dpf (Fig. 2.2B; $p = 0.7047$). Eos from the AP cell transgene labeled about 6% of hair cells at both 5 and 8 dpf (Fig. 2.2D; $p = 0.9668$). Since there is no change over the three-day span, neither of these populations are responsible for generating new hair cells under homeostatic conditions. In contrast, the amount of hair cells labeled with photoconverted Eos from the DV cell transgene increased from 39% to 56% over that three-day span (Fig. 2.2F; $p < 0.0001$). Thus, the DV cell population seems to be predominantly involved in ongoing hair cell generation during homeostasis.

We next used these transgenic lines to determine whether there was any functional difference between these support cell subpopulations regarding their ability to serve as hair cell progenitors during regeneration. Each of the nlsEos lines were once again crossed to brn3c:GFP fish in order to distinguish hair cell nuclei. Eos in support cells was photoconverted at 5 dpf, and larvae were subjected to neomycin-induced hair cell ablation and then fixed and immunostained for GFP at 72 hpt (Fig. 2.3A). Only 4% of regenerated hair cells were derived from the Peripheral cell population, whereas the AP cell and DV cell populations contributed significantly more, generating 20% and 61% of regenerated hair cells, respectively (Fig. 2.3B-D, arrowheads; Fig. 3E; $p = 0.003$ [Peripheral vs. AP], $p < 0.0001$ [Peripheral/AP vs. DV]). In order to ensure that this difference in Eos incorporation was not simply due to relative proportion of available Eos-positive support cells, we counted the number of Eos-positive support cells in each transgenic line at 5 dpf, prior to hair cell ablation. There were about half as many Peripheral cells relative to the other two populations, but no significant difference between the number of AP cells and the number of DV cells (Fig. 2.3F; Peripheral = 14.30 ± 4.17; AP = 22.8 ± 4.40; DV =

23.86 ± 4.45; $p < 0.0001$ [Peripheral vs. AP/DV], $p > 0.9999$ [AP vs. DV]). Thus, the difference in regenerative capacity between these populations is not simply a reflection of the number of available cells, but rather of differences in the progenitor identity of the populations.

2.3.3 Inhibition of Notch Signaling Differentially Impacts Support Cell Subpopulations

Notch-mediated lateral inhibition plays a crucial role in ensuring the proper number of hair cells are regenerated, and inhibition of Notch signaling following hair cell damage dramatically increases the number of regenerated hair cells (Ma et al., 2008; Romero-Carvajal et al., 2015; Wibowo et al., 2011). Thus, we examined how Notch inhibition impacted the progenitor function of our three support cell populations. We crossed all of our nlsEos lines to the brn3c:GFP line, and treated double-positive larvae with 50 μM LY411575 (LY), a potent γ-secretase inhibitor (Mizutari et al., 2013; Romero-Carvajal et al., 2015), for 24 hours immediately following neomycin treatment. Fish were fixed at 72 hpt and immunostained for GFP. In all three lines, after Notch inhibition (Neo/LY) there were roughly twice as many hair cells as control fish (Neo) (Fig. 2.4A-B, E-F, I-J; $p < 0.0001$ [all lines]), consistent with previous studies. The small number of Peripheral cell-derived hair cells was no different between LY-treated fish and non-treated fish (Fig. 2.4C; 0.62 ± 1.28 [Neo] vs. 1.15 ± 2.16 [Neo/LY]; $p = 0.2481$). By contrast, the number of nlsEos-positive hair cells from both AP and DV cells increased in fish treated with LY. Moreover, while the number of nlsEos-positive hair cells derived from DV cells doubled in LY-treated fish (Fig. 2.4K; 7.40 ± 2.13 [Neo] vs. 15.25 ± 6.36 [Neo/LY]; $p < 0.0001$), those derived from AP cells increased roughly five-fold (Fig. 2.4G; 2.22 ± 1.94 [Neo] vs. 11.38 ± 4.23 [Neo/LY]; $p < 0.0001$). As a consequence, the percentage of hair cells derived from DV cells decreased correspondingly (Fig. 2.4L; 67.86 ± 14.63 [Neo] vs. 54.69

± 14.01 [Neo/LY]; $p < 0.0001$), whereas those derived from AP cells doubled (Fig. 2.4H; 25.19 ± 21.72 [Neo] vs. 50.68 ± 19.23 [Neo/LY]; $p < 0.0001$). These data suggest that generation of hair cells from both the AP and DV populations is regulated by Notch signaling (with the AP population being regulated to a greater extent), whereas Peripheral cells are not responsive to Notch signaling.

2.3.4 Selective Ablation of DV Cells Reduces Hair Cell Regeneration

Since the DV cell population generates roughly 60% of regenerated hair cells, we sought to determine whether these cells were required for hair cell regeneration. To this end, we generated a transgenic line in which an enhanced-potency nitroreductase (epNTR; Tabor et al., 2014) fused to GFP was introduced into the *sost* locus using CRISPR (Tg[*sost*:epNTR-GFP]^{w216}, hereafter known as *sost*:NTR-GFP). Nitroreductase is a bacterial enzyme that selectively binds its prodrug Metronidazole (Mtz), converting Mtz into toxic metabolites that kill the cells expressing it (Curado et al., 2007). We then compared the extent of *sost:NTR-GFP* expression in DV cells, as defined by the *sost:nlsEos* transgene. At 3 dpf, soon after the initiation of transgene expression, we see considerable overlap between NTR-GFP and nlsEos. All NTR-GFP+ cells were also positive for nlsEos, while an additional subset of cells expressed nlsEos alone. When we compared expression at 5 dpf, the size of the double-positive (NTR-GFP+; nlsEos+) population did not change, whereas the number of cells expressing nlsEos alone increased significantly, occupying a more central location (Fig. 2.5A-B, arrowheads; Fig. 2.5C; NTR-GFP/nlsEos: 9.04 ± 2.39 [3 dpf] vs. 8.47 ± 2.27 [5 dpf]; nlsEos only: 6.10 ± 2.27 [3 dpf] vs. 10.86 ± 2.72 (5 dpf); $p > 0.9999$ [NTR-GFP/nlsEos], $p < 0.0001$ [nlsEos only]). These observations are consistent with the idea that both transgenes initiate expression at the same

time, but that nlsEos protein is retained longer than NTR-GFP protein as cells mature and as a result, NTR-GFP is expressed in a subset of DV cells. We next tested to the efficacy of DV cell ablation at 3 and 5 dpf. Treatment of these fish with 10 mM Mtz for 8 hours was sufficient to ablate the majority of NTR-GFP cells. Treating fish with Mtz for 8 hours at 5 dpf (Mtz5) slightly but significantly decreased the number of support cells solely expressing nlsEos by about 13%. Treating fish with Mtz for 8 hours at 3 dpf, followed by a second 8-hour Mtz treatment at 5 dpf (Mtz3/5) decreased the number of solely nlsEos-positive cells even further, by about 40% (Fig. 2.5D-G; Mock: 11.18 ± 2.04; Mtz5: 9.72 ± 2.03; Mtz3/5: 6.76 ± 2.12; $p = 0.0288$ [Mock vs. Mtz5], $p < 0.0001$ [Mock vs. Mtz3/5, Mtz5 vs. Mtz3/5]).

We next tested the impact of DV cell ablation on hair cell regeneration. We compared two groups: neomycin exposure followed by Mtz treatment at 5 dpf (Neo/Mtz5), compared to Mtz treatment at 3 dpf, then neomycin treatment at 5 dpf followed by a second Mtz treatment (Mtz3/Neo/Mtz5; Fig. 2.6A). For both groups, nlsEos was photoconverted at 5 dpf, just prior to neomycin treatment, and larvae were fixed at 72 hpt and immunostained for GFP and Parvalbumin (to label NTR-GFP+ cells and hair cells, respectively). The Neo/Mtz5 treatment resulted in a small but significant reduction in both hair cells and nlsEos-positive hair cells per neuromast relative to normal regeneration (Fig. 2.6B-C, E-F; Total hair cells: 11.73 ± 2.10 [Neo] vs. 9.33 ± 1.88 [Neo/Mtz5]; $p = 0.0001$; nlsEos+ hair cells: 7.78 ± 2.36 [Neo] vs. 4.90 ± 2.02 [Neo/Mtz5]; $p = 0.0003$). The Mtz3/Neo/Mtz5-treated larvae exhibited even fewer hair cells per neuromast (Fig. 2.6D, E; 11.73 ± 2.10 [Neo] vs. 7.52 ± 1.74 [Mtz3/Neo/Mtz5]; $p < 0.0001$), with nlsEos-labeled hair cells decreased to a mere 14% of total regenerated hair cells (Fig. 2.6G; 65.81 ± 14.89 [Neo] vs. 14.29 ± 18.10 [Mtz3/Neo/Mtz5]; $p < 0.0001$). Importantly, Mtz treatment of siblings without the *sost:*NTR-GFP transgene had no impact on hair cell

regeneration (Supplemental Fig. 2.14; Neo: 9.5 ± 1.50; Mtz3/Neo/Mtz5: 9.98 ± 1.51; p = 0.2317). Thus, ablation of DV cells reduces the number of hair cells regenerated.

We then examined how Notch signaling impacted hair cell regeneration in the context of DV cell ablation. We treated *sost*:NTR-GFP larvae with 50 μM LY for 24 hours following ablation (Mtz3/Neo/Mtz5/LY) and assayed hair cell number at 72 hpt (Fig. 2.7A). As expected, the number of regenerated hair cells increased significantly after LY treatment in all groups (Fig. 2.7B-F; $p < 0.0001$), and DV cell ablation significantly decreased hair cell regeneration (Fig. 2.7B, D, F; 9.42 ± 1.85 [Neo] vs. 6.86 ± 1.76 [Mtz3/Neo/Mtz5]; p = 0.0058). However, LY treatment following Mtz ablation resulted in significantly fewer regenerated hair cells than LY alone (Fig. 2.7C, E, F; 21.08 ± 4.42 [Neo/LY] vs. 15.06 ± 3.51 [Mtz3/Neo/Mtz5/LY]; p = 0.0029), indicating that inhibiting Notch signaling cannot fully compensate for the loss of the DV population.

2.3.5 AP and DV Cells Define Separate Progenitor Populations

While the DV population generates roughly 60% of hair cells after damage, the other 40% must derive from a different population. Consistent with this observation, reduction of DV cells by Mtz treatment only partially blocks new hair cell formation, indicating that there must be additional progenitor populations. We believed that AP cells could define this additional population, since they were capable of generating roughly 20% of regenerated hair cells (Fig. 2.3E). However, there may be some overlap between the expression of *tnfsf10l3*:nlsEos defining the AP domain and *sost*:nlsEos defining the DV domain. When we crossed the *tnfsf10l3*:nlsEos and *sost*:nlsEos lines together, we found that roughly 88% of regenerated hair cells were nlsEos positive when larvae expressed both transgenes, compared to 65% from *sost*:nlsEos alone and

28% from *tnfsf10l3*:nlsEos alone (Fig. 2.8A-E; $p < 0.0001$). Thus, while not completely additive, these data suggest that the AP population is distinct from the DV population in terms of its progenitor function.

We next examined how the AP population would respond to the ablation of the DV population. We crossed the *tnfsf10l3*:nlsEos line to the *sost*:NTR-GFP line, sorted out double-positive larvae, and compared normal regeneration to that after Mtz treatment (Mtz3/Neo/Mtz5, since this had served to be the best treatment paradigm). As above, nlsEos was photoconverted at 5 dpf, immediately prior to neomycin treatment, and larvae were fixed at 72 hpt and immunostained for GFP and Parvalbumin. Mtz-ablated larvae had significantly fewer hair cells than non-ablated larvae, as in previous experiments (Fig. 2.9C; 10.36 ± 1.60 [Neo] vs. 7.98 ± 1.74 [Mtz3/Neo/Mtz5]; $p < 0.0001$), but the number of nlsEos-postive hair cells was no different between the two groups (Fig. 2.9A-B, arrowheads; Fig. 2.9D; 2.88 ± 1.83 [Neo] vs. 3.14 ± 1.43 [Mtz3/Neo/Mtz5]; $p = 0.3855$). The percentage of Eos-positive hair cells did increase, but this is only because the total number of hair cells decreased overall (Fig. 2.9E; 27.26 ± 16.00 [Neo] vs. 40.43 ± 19.44 [Mtz3/Neo/Mtz5]; $p = 0.0002$). Thus, the AP population's progenitor function remains unchanged following DV ablation, providing further support that it is a separate progenitor population from the DV population.

2.3.6 The DV Population Regenerates from Other Support Cell Subpopulations

When examining hair cell regeneration following DV cell ablation, we consistently noticed that there was an increase in NTR-GFP+ cells at 72 hpt. This led us to hypothesize that DV cells were capable of regeneration even in the absence of hair cell damage. To test this, we first administered a 48-hour pulse of EdU (changing into fresh EdU solution after the first 24

hours) immediately following Mtz ablation at 5 dpf and fixed immediately after EdU washout. At 48 hours post ablation, we observed slightly more than half the number of the NTR-GFP+ cells relative to unablated larvae (Fig. 2.10C; 8.94 ± 1.62 [Mock] vs. 5.34 ± 2.14 [Mtz]; $p < 0.0001$). However, 58% of NTR-GFP+ cells were EdU-positive in fish treated with Mtz, compared to just 15% in unablated larvae (Fig. 2.10A-B, arrowheads; Fig. 2.10D; $p < 0.0001$). These results indicate that new DV cells arise from proliferation.

To determine the source of new DV cells, we crossed *sost*:NTR-GFP fish to our three different nlsEos lines. Double-transgenic fish were photoconverted at 5 dpf, Mtz-ablated, and then fixed at 72 hpt and immunostained for GFP. Following ablation, 56% of NTR-GFP+ cells expressed photoconverted nlsEos when DV cells were labeled, compared to 97% in unablated controls (Fig. 2.11A-B, arrowheads; Fig. 2.11C; $p < 0.0001$). 31% of NTR-GFP+ cells expressed photoconverted nlsEos when Peripheral cells were labeled, compared to 6% in controls (Fig. 2.11D-E, arrowheads; Fig. 2.11F; $p < 0.0001$) and 21% of NTR-GFP+ cells expressed photoconverted nlsEos when AP cells were labeled, compared to 7% in controls (Fig. 2.11G-H, arrowheads; Fig. 2.11I; $p = 0.0004$). Thus, DV cells are capable of being replenished after Mtz ablation by other DV cells as well as by both AP and Peripheral cells.

2.4 Discussion

2.4.1 Differences in Hair Cell Progenitor Identity Among Support Cell Populations

The data shown above indicate that there are at least three spatially and functionally distinct progenitor populations within the neuromast: (1) a highly regenerative, dorsoventral (DV) population, marked by *sost*:nlsEos, which generates the majority of regenerated hair cells; (2) an anteroposterior (AP) population, marked by *tnfsf10l3*:nlsEos, which also contributes to

hair cell regeneration albeit to a far lesser extent than *sost;* and (3) a peripheral population (Peripheral), marked by *sfrp1a*:nlsEos, that does not contain hair cell progenitors (Fig. 2.12). This model of high regenerative capacity in the dorsoventral region and low regenerative capacity in the anteroposterior region is consistent with the label-retaining studies performed by Cruz et al., (2015) as well as the BrdU-localization studies of Romero-Carvajal et al., (2015). However, an examination of the overlap in expression between *sost*:nlsEos and *sost*:NTR-GFP reveals distinctions even amongst this DV progenitor population. We hypothesize that cells that express only nlsEos have matured from those that express both NTR-GFP and nlsEos. We posit that these more mature nlsEos cells serve as hair cell progenitors. Consistent with this idea, Mtz treatment at 5 dpf that spares nlsEos cells not expressing NTR-GFP has only a small effect on hair cell regeneration while Mtz treatment at both 3 and 5 dpf results in substantial reduction in hair cell regeneration.

While we have identified distinct hair cell progenitor populations (DV and AP), these populations do not account for all of the hair cell progenitors in the neuromast. The combination of these cells generated 88% of new hair cells, meaning that the remaining 12% were derived from other sources. Furthermore, the AP population only accounted for 40% of new hair cells generated after neomycin treatment following DV cell ablation. Thus, there must be some other population (or populations) of support cells that are serving as hair cell progenitors that we have not labeled with our transgenic techniques. The best candidates for this role are centrally located support cells found ventral to hair cells, although the identity of these cells remains to be determined.

2.4.2 The Role of Planar Cell Polarity and Progenitor Localization

Neuromasts located on the trunk develop at different times from different migrating primordia. Within a given neuromast, hair cells are arranged such that their apical stereocilia respond to directional deflection in one of two directions along the body axis. Hair cells derived from the first primordium (primI) respond along the anteroposterior axis, and hair cells derived from the second primordium (primII) respond along the dorsoventral axis (López-Schier & Hudspeth, 2006; López-Schier, Starr, Kappler, Kollmar, & Hudspeth, 2004). Spatial restriction of support cell proliferation is orthogonal to hair cell planar polarity, with proliferation occurring dorsoventrally in primI-derived neuromasts and anteroposteriorly in primII-derived neuromasts (Romero-Carvajal et al., 2015). This 90-degree switch between prim1- and primII-derived neuromasts is reflected in the distribution of labeled cell populations as well: *tnfsf10l3*:nlsEos and *sost*:nlsEos retain their asymmetric localization in primII-derived neuromasts, but *tnfsf10l3*:nlsEos is predominantly expressed in the dorsoventral region and *sost*:nlsEos is restricted to the anteroposterior region (data not shown). *Sfrp1a*:nlsEos expression remains limited to the periphery. Thus, within a given neuromast along the trunk, expression of *sost*:nlsEos is orthogonal to hair cell planar polarity, and that of *tnfsf10l3*:nlsEos is parallel to hair cell planar polarity.

The relationship between asymmetric progenitor localization and hair cell planar polarity remains unknown. Planar cell polarity (PCP) signaling often drives asymmetry in other tissues and has been implicated in the planar polarity of lateral line hair cells. Zebrafish deficient in Vangl2, a critical component of the PCP pathway, still develop neuromasts, but their hair cells are oriented randomly toward one another and do not respond along a single axis (López-Schier & Hudspeth, 2006). Furthermore, this random orientation stems from misaligned divisions of

hair cell progenitors (Mirkovic et al., 2012). The transcription factor Emx2 has also been recently implicated in determining hair cell planar polarity (Jiang, Kindt, & Wu, 2017). Whether these genes or other components of PCP signaling mediate the asymmetric expression of *sost*:nlsEos and *tnfsf10l3*:nlsEos remains to be determined. It would also be interesting to examine whether hair cell planar polarity is influenced by the asymmetric localization of these progenitor populations, or vice versa.

2.4.3 Regeneration of Support Cells in the Absence of Hair Cell Damage

Since zebrafish are able to properly regenerate their hair cells after multiple successive insults (I. A. Cruz et al., 2015; Pinto-Teixeira et al., 2015), and both daughters of progenitors give rise to hair cells, there must be a means of replenishing hair cell progenitors. Our EdU/BrdU double labeling experiment qualitatively demonstrated that hair cell progenitors could be replenished via proliferation of other support cells. It was thus unsurprising that DV cells could themselves regenerate. It is notable, however, that DV cells could be replenished even in the absence of hair cell damage, which means that hair cell death is not the sole signal that triggers support cell proliferation. Support cell regeneration in the absence of hair cell death has been observed in mammals, as certain types of cochlear support cells (inner border cells and inner phalangeal cells) are capable of regeneration following selective ablation, a process that occurs via transdifferentiation (Mellado Lagarde et al., 2014). In contrast, zebrafish DV cell regeneration primarily occurs via proliferation, as a majority of new DV cells were EdU-positive following Mtz-induced ablation. DV cells that were not EdU-positive could have arisen after the EdU pulse, been retained due to incomplete ablation, or potentially resulted from transdifferentiation from another source.

All three labeled support cell populations were able to replenish DV cells following Mtz-induced ablation. DV cells themselves contributed nearly 60% of new DV cells, although we cannot rule out that this number is inflated due to incomplete ablation. This result suggests that DV cells choose to either generate new hair cells or replenish lost DV cells, undergoing a form of self-renewal that does not require asymmetric division. The AP population is also capable of replenishing DV cells. That both of these populations can generate new DV cells is consistent with recent findings from Viader-Llargués et al., (2018). This study defined support cells as a peripheral mantle population and a central sustentacular population. Following laser ablation of large portions of the neuromast, they found that sustentacular cells were able to regenerate mantle cells and other sustentacular cells, as well as hair cells, and could thus be considered tripotent progenitors. The transgenic lines they used to label sustentacular cells were broadly expressed, and thus should encompass both AP and DV populations. While we have not been able to selectively ablate the Peripheral cell population, and therefore cannot test whether DV and AP populations can generate them, the DV and AP populations can both generate new hair cells and new DV cells, indicating that they are both at least bipotent.

We found that the Peripheral population could also generate new DV cells following Mtz-induced ablation. Furthermore, it contributes more to DV regeneration than does the AP population. This was especially surprising since proliferation has rarely been observed in peripheral cells, at least during normal hair cell regeneration (Ma et al., 2008; Romero-Carvajal et al., 2015). However, the loss of a progenitor population could be considered to be a case of extreme damage to the neuromast, thus prompting the Peripheral cell population to respond. That Peripheral cells can serve as progenitors only in extreme circumstances is consistent with the findings of Romero-Carvajal et al., 2015 and Viader-Llargués et al., 2018. Both studies

suggested that mantle cells are capable of regenerating other cell types in the neuromast following extreme damage. However, the latter study found that mantle cells could only generate other mantle cells. Whether the Peripheral cell population in particular is capable of doing the same remains to be tested. Mantle cells have also been shown to proliferate following tail amputation, forming a migratory placode that forms new neuromasts along the regenerated tail (Dufourcq et al., 2006; Jones & Corwin, 1993). Given the differences across studies, we have hesitated to designate the *sfrp1a*:nlsEos labeled cells as mantle cells and have instead adopted the "Peripheral" label. Since Peripheral cells can generate hair cell progenitors, we have characterized them as “upstream progenitors” (Fig. 2.12).

The zebrafish lateral line system continues to grow through larval and adult stages (Ledent, 2002; Nuñez et al., 2009; Sapède, Gompel, Dambly-Chaudière, & Ghysen, 2002), with new neuromasts formed from budding from extant neuromasts (Nuñez et al., 2009; Wada, Ghysen, et al., 2013; Wada, Dambly-Chaudière, Kawakami, & Ghysen, 2013) and generated anew from interneuromast cells, latent precursors deposited between neuromasts by the migrating primordium (Grant, Raible, & Piotrowski, 2005; Nuñez et al., 2009). We note that the *sfrp1a*:nlsEos transgene is expressed in interneuromast cells as well as Peripheral neuromast cells. Whether these cells share similar properties to generate new neuromasts remains to be tested.

Our model of neuromast progenitor identity does bear some similarities with other regenerative tissues. Both the hair follicle and intestinal epithelium contain a niche of stem cells (bulge cells and crypt cells, respectively) which generate transit-amplifying cells that are able to generate other cell types (Barker et al., 2007; Ito et al., 2005; Taylor, Lehrer, Jensen, Sun, & Lavker, 2000). Due to their high rate of proliferation and multipotency, the DV cells in the

neuromast could be likened to these transit-amplifying cells. However, progenitors in the neuromast may bear the most similarity to those of the olfactory epithelium, which contains two distinct progenitor populations: globose basal cells (GBCs), which are transit-amplifying cells that can restore lost olfactory neurons; and horizontal basal cells (HBCs), a quiescent population that can generate multiple cell types, including GBCs, in instances of extreme damage (Iwai, Zhou, Roop, & Behringer, 2008; Leung, Coulombe, & Reed, 2007). In our model, the DV and Peripheral cells are comparable to the GBCs and HBCs, respectively. However, we cannot make the claim that the Peripheral population is a resident stem cell population (like bulge cells, crypt cells, and HBCs), as we do not yet know if it is capable of self-renewal or of generating every cell type within the neuromast.

2.4.4 Notch Signaling Differentially Regulates Support Cell Populations

Inhibition of Notch signaling during hair cell regeneration significantly increased the number of hair cells derived from both DV and AP cells, which was not unexpected given that both are hair cell progenitor populations. However, Notch inhibition had a greater impact on the AP population than on the DV population, suggesting that it may be more strongly regulated by Notch signaling. The receptor *notch3*, in particular, is most strongly expressed in the anteroposterior portions of the neuromast (Romero-Carvajal et al., 2015; Wibowo et al., 2011). Furthermore, a transgenic reporter of Notch activity is also expressed in the anteroposterior region (Romero-Carvajal et al., 2015; Wibowo et al., 2011). It is thus likely that asymmetrically-localized Notch signaling maintains quiescence among AP cells during homeostasis and is responsible for suppressing the contribution of the AP population to hair cell regeneration (compared to DV contribution). Since Notch signaling is not as strong in the dorsoventral

regions of the neuromast, the DV population is less affected and could already be more "primed" to serve as hair cell progenitors than the AP population.

Notch inhibition did not have any impact on the Peripheral population's contribution to hair cell regeneration, indicating that Notch signaling does not suppress hair cell production by Peripheral cells. While it is difficult to tell from *in situ* expression, it seems that the Notch reporter is not active in the peripheral mantle cells (Romero-Carvajal et al., 2015; Wibowo et al., 2011). Thus, there must be some other mechanism, either intrinsic or extrinsic, that maintains relative quiescence among the Peripheral population.

It is not clear why these distinct populations of progenitors exist, as there is no clear difference in the types of hair cells they produce. Hair cells polarized in opposing direction are daughters of the final division of the hair cell progenitor (López-Schier & Hudspeth, 2006). Heterogeneity has also been recently described in the synaptic responses of lateral line hair cells (Zhang et al., 2018), but these differences appear lineage-independent. Instead, the allocation of distinct progenitors may serve an advantage with respect to their differential regulation. For example, our data suggest that DV cells contribute more to homeostatic addition of new hair cells to the neuromast in the absence of damage, while both AP and DV cells are engaged after hair cell damage. AP cells were unable to overcome the loss of the DV population, suggesting that feedback mechanisms regulating both hair cell production and progenitor replacement operate independently. While both AP and DV populations are regulated by Notch signaling, this regulation appears to operate independently as Notch inhibition does not compensate for DV ablation. Independent progenitors may offer the flexibility to add new hair cells under a variety of conditions for both ongoing hair cell turnover and in the face of catastrophic hair cell loss.

2.5 Materials and Methods

Fish Maintenance

Experiments were conducted on 5-8 dpf larval zebrafish (except for the double hair cell ablation experiment, which was conducted on 15-18 dpf fish). Larvae were raised in E3 embryo medium (14.97 mM NaCl, 500 μM KCL, 42 μM Na_2HPO_4, 150 μM KH_2PO_4, 1 mM $CaCl_2$ dihydrate, 1 mM $MgSO_4$, 0.714 mM $NaHCO_3$, pH 7.2) at 28.5°C. All wildtype animals were of the AB strain. Zebrafish experiments and husbandry followed standard protocols in accordance with University of Washington Institutional Animal Care and Use Committee guidelines.

Plasmid Construction

The myo6b:mKate2 construct was generated via the Gateway Tol2 system (Invitrogen). A pME-mKate2 (the mKate2 sequence being cloned from pMTB-Multibow-mfR, Addgene #60991) construct was generated via BP Recombination, and then a pDEST-myo6b:mKate2 construct was generated via LR recombination of p5E-myo6b, pME-mKate2, p3E-pA, and pDEST-iTol2-pA2 vectors. The mbait-GFP construct was a gift from Shin-Ichi Higashijima's lab. The mbait-nlsEos construct was also generated via Gateway LR recombination of p5E-mbait/HSP70l, pME-nlsEos, p3E-pA, and pDEST-iTol2-pA2 vectors. The mbait-epNTR-GFP construct was generated via Gibson assembly, inserting the coding sequence of epNTR (cloned from pCS2-epNTR obtained from Harold Burgess' lab) plus a small linker sequence in front of the GFP in the original pBSK mbait-GFP vector. All plasmids were maxi prepped (Qiagen) prior to injection.

CRISPR Guides

Gene-specific guide RNA (gRNA) sequences were as follows:

sfrp1a: GTCTGGCCTAAAGAGACCAG

tnfsf10l3: GGGCTTGTATAGGAGTCACG

sost: GGGAGTGAGCAGGGATGCAA

GGGCGAAGAACGGTGGAAGG

All gRNAs were synthesized according to the protocol outlined in (Shah, Davey, Whitebirch, Miller, & Moens, 2015), but were purified using a Zymo RNA Clean & Concentrator kit. Upon purification, gRNAs were diluted to 1 μg/μL, aliquoted into 4 μL aliquots, and stored at -80°C. *Sfrp1a* and *tnfsf10l3* gRNA sequences were designed via http://crispr.mit.edu, and the *sost* gRNA sequences were designed via http://crisprscan.org. The *tnfsf10l3* gRNA was targeted upstream of the gene's start ATG codon, whereas the *sfrp1a* and *sost* guides were targeted to exons.

Tol2 Transgenesis

The Tg[myo6b:mKate2]^{w218} (hereafter called myo6:mKate2) line was generated via Tol2 transgenesis. 1-2 nL of a 5 μL injection mix consisting of 20 ng/μL myo6b:mKate2 plasmid, 40 ng/μL transposase mRNA, and 0.2% phenol red were injected into single cell wildtype embryos. Larvae were screened for expression at 3 dpf and transgenic F_0 larvae were grown to adulthood. F_0 adults were outcrossed to wildtype fish, transgenic offspring were once again grown to adulthood, and the resulting adults were used to maintain a stable line.

CRISPR-mediated Transgenesis

All support cell transgenic lines were generated via CRISPR-mediated transgenesis. For most injections, a 5 μL injection mix was made consisting of 200 ng/μL gene-specific gRNA, 200 ng/μL mbait gRNA, 800 ng/μL Cas9 protein (PNA Bio #CP02), 20 ng/μL mbait-reporter plasmid, and 0.24% phenol red. The gRNAs and Cas9 protein were mixed together first, then heated at 37°C for 10 minutes, after which the other components were added. In the case of *sost*, in which two gRNAs were co-injected, each gRNA was added to the mix at a final concentration of 100 ng/μL (so 200 ng/μL of total guide-specific gRNA). When reconstituting the Cas9 protein, DTT was added to a final concentration of 1 mM DTT. This is highly recommended to reduce needle clogging during the injection process!! 1-2 nL of these injection mixes were injected into single cell wildtype embryos. Larvae were screened for expression at 3 dpf and transgenic F_0 larvae were grown to adulthood. F_0 adults were outcrossed to wildtype fish, transgenic offspring were once again grown to adulthood, and the resulting adults were used to maintain a stable line.

Photoconversion

In order to photoconvert multiple nlsEos fish at once, larvae were transferred to a 60 x 15mm petri dish and placed in a freezer box lined with aluminum foil. Then, an iLumen 8 UV flashlight (procured from Amazon) was placed over the dish and turned on for 15 minutes. Following the UV pulse, larvae were returned to standard petri dishes to await experimentation.

Drug Treatments

For all drug treatments, zebrafish larvae were placed in baskets in 6 well plates to facilitate transfer of larvae between media. Larvae were treated at 5 dpf unless otherwise noted. All wells contained 10 mL of drug, E3 embryo medium with the same effective % DMSO as the drug (for mock treatments), or plain E3 embryo medium for washout. Following treatment, the fish were washed twice into fresh E3 embryo medium by moving the baskets into adjacent wells in the row, then washed a third time by transferring them into a 100 mm petri dish with fresh E3 medium. All drugs were diluted in E3 embryo medium. The drug treatment paradigms were as follows: for hair cell ablation, 400 μM neomycin (Sigma) for 30 minutes; for *sost*:NTR ablation, 10 mM metronidazole (Mtz; Sigma) with 1% DMSO; for Notch inhibition, 50 μM LY411575 (LY; Sigma) for 24 hours; for the *sost* ablation/Notch inhibition experiment (Fig. 10): 10mM Mtz/50 μM LY for 8 hours, then 50 μM LY for 16 hours.

For double hair cell ablation studies, larvae that were treated with neomycin were raised on a nursery in the UW fish facility beginning at 7 dpf and then treated with 400 μM neomycin again at 15 dpf in standard petri dishes (10 days following the first neomycin treatment). These juvenile fish were washed into fresh system water multiple times before being returned to the nursery and were then fixed three days later (18 dpf).

EdU and BrdU Treatments

Following hair cell ablation with neomycin, larvae were incubated in 500 μM F-ara-EdU (Sigma #T511293) for 24 hours. Following *sost*:NTR ablation with Mtz, larvae were incubated in the same concentration of EdU for 48 hours. Larvae were placed into fresh EdU after the first 24

hours. F-ara-EdU was originally reconstituted in 50% H_2O and 50% DMSO to 50 mM, so the working concentration of DMSO of 500 μM was 0.5%. In the case of the double ablation studies, juvenile fish were incubated in 10mM BrdU (Sigma) with 1% DMSO in system water (used in the UW fish facility) following the second neomycin treatment for 24 hours. Following treatment, larvae were washed in fresh system water several times.

Immunohistochemistry

Zebrafish larvae were fixed in 4% paraformaldehyde in PBS containing 4% sucrose for either 2 hours at room temperature or overnight at 4°C. Larvae were then washed 3 times (20 minutes each) in PBS containing 0.1% Tween20 (PBT), incubated for 30 minutes in distilled water, then incubated in antibody block (5% heat-inactivated goat serum in PBS containing 0.2% Triton, 1% DMSO, 0.02% sodium azide, and 0.2% BSA) for at least one hour at room temperature. Larvae were then incubated in mouse anti-parvalbumin or rabbit anti-GFP (or sometimes both simultaneously) diluted 1:500 in antibody block overnight at 4°C. The next day, larvae were once again washed 3 times (20 minutes each) in PBT, then incubated in a fluorescently-conjugated secondary antibody (Invitrogen, Alexa Fluor 488, 568, and/or 647) diluted 1:1000 in antibody block for 4-5 hours at room temperature. From this point onward, larvae were protected from light. Larvae were then rinsed 3 times (10 minutes each) in PBT and then stored in antibody block at 4°C until imaging. For BrdU immunohistochemistry, juvenile fish were rinsed once in 1N HCl, then incubated in 1N HCl following washout of Click-iT reaction mix (see below). IHC proceeded as above, except that the antibody block contained 10% goat serum and the fish were incubated in mouse anti-BrdU at a dilution of 1:100. All wash and incubation steps occurred with rocking.

Click-iT

Cells that had incorporated F-ara-EdU were visualized via a Click-iT reaction. In the case of the double hair cell ablation experiment, Click-iT was performed before immunohistochemistry. Following fixation, fish were washed 3 times (10 minutes each) in PBT, then permeabilized in PBS containing 0.5% Triton-X for 30 minutes, then washed another 3 times (10 minutes each) in PBS. Next, fish were incubated for 1 hour at room temperature in a Click-iT reaction mix consisting of 2mM $CuSO_4$, 10 μM Alexa Fluor 555 azide, and 20 mM sodium ascorbate in PBS (made fresh). Fish were protected from light from this point onwards. Afterwards, the standard IHC protocol listed above was performed (beginning with the 3 20-minute washes in PBT). For the *sost*:NTR regeneration experiment, the Click-iT reaction was performed after IHC. Following incubation in secondary antibody, larvae were washed 3 times (10 minutes each) in PBS, then incubated in 700 μL of the Click-iT reaction mix (again, made immediately prior to incubation) for 1 hour at room temperature. Larvae were then washed 6 times (20 minutes each) in PBT to ensure proper clearing of background labeling and stored in antibody block at 4°C until imaging.

Confocal Imaging

With the exception of imaging requiring a far-red laser (Fig. 1F-N, Fig. 3C-I, Fig. 5), all imaging was performed using an inverted Marianas spinning disk system (Intelligent Imaging Innovations, 3i) with an Evolve 10 MHz EMCCD camera (Photometrics) and a Zeiss C-Apochromat 63x/1.2W numerical aperture water objective. All imaging experiments were conducted with fixed larvae ages 5-8 dpf. Fish were placed in a chambered borosilicate

coverglass (Lab-Tek) containing 2.5-2.5 mL E3 embryo medium and oriented on their sides with a slice anchor harp (Harvard Instruments). Imaging was performed at ambient temperature, generally 25°C. Fish were positioned on their sides against the cover glass in order to image the first 5 primary neuromasts of the posterior lateral line (P1-P5). All imaging was performed with an intensification of 650, a gain of 3, an exposure time between 25-1500 ms (depending on the brightness of the signal) for 488, 561, and 405 lasers, and a step size of 1 μm. All 3i Slidebook images were exported as .tif files to Fiji.

In cases when a far-red laser was required, imaging was performed on a Zeiss LSM 880 microscope with a Zeiss C-Apochromat 40x/1.2W numerical water objective. Fish were immersed in a solution of 50%glycerol/50% PBS, and then mounted on a plain microscope slide (Richard-Allen) beneath a triple wholemount coverslip. Imaging was performed at ambient temperature, generally 25°C. Fish were positioned on their sides against the cover glass in order to image the first 5 primary neuromasts of the posterior lateral line (P1-P5). For the double hair cell ablation experiment, following fixation the tails of fish were cut off and mounted underneath a single wholemount coverslip. The 3 neuromasts of the terminal cluster were imaged per tail. All imaging was performed at 4-5x digital zoom with master gain between 500-800 for 488, 561, and 647 lasers, and a step size of 1 μm. All images were captured through the Zen Black software and opened in Fiji as .czi files.

Statistical Analysis

All statistical analyses were done with GraphPad Prism 6.0. The Mann Whitney U test was used for comparisons between 2 groups, whereas the Kruskal-Wallis test, with a Dunn's post-test, was used for comparisons between 3 or more groups. Statistical significance was set at $p = 0.05$.

2.6 Acknowledgements

We would like to thank David White and the staff of the UW Fish Facility for animal care and maintenance, Ivan Cruz for providing the *sost* gRNA, Shin-Ichi Higashijima for the mbait-GFP vector, Harold Burgess for the pCS2-epNTR vector, Madeleine Hewitt for assistance with data analysis, and Sarah Pickett for critical reading of the manuscript.

2.7 Figures

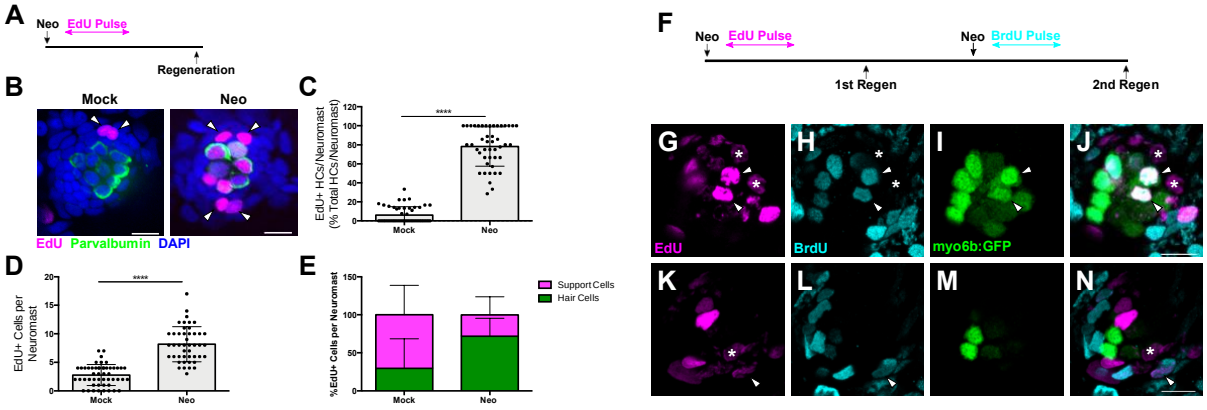

Figure 2.1. Hair cell progenitors are replenished via proliferation of other support cells. **(A, F)** Timelines of single-ablation (A) and double-ablation (F) proliferation experiments. **(B)** Maximum projections of mock- (Mock) and neomycin-treated (Neo) neuromasts. EdU-positive cells are shown in magenta, anti-Parvalbumin-stained hair cells are shown in green, and DAPI-stained nuclei are shown in blue. Arrowheads indicate EdU-positive support cells. Scale bar = 10 μm. **(C)** Percentage of hair cells per neuromast labeled by EdU. Mock: 6.11 ± 8.69, n = 50 neuromasts; Neo: 78.24 ± 20.69, n = 45 neuromasts; mean ± SD; Mann Whitney U test, $p < 0.0001$. **(D)** Total EdU-positive cells per neuromast. Mock: 2.78 ± 1.84, n = 50 neuromasts; Neo: 8.18 ± 3.07, n = 45 neuromasts; mean ± SD; Mann Whitney U test, $p < 0.0001$. **(E)** Percentage of EdU-positive cells per neuromast that are either hair cells or support cells. Mock: 29.73% hair cells, 70.27% support cells, n = 50 neuromasts; Neo: 72.02% hair cells, 27.98% support cells, n = 45 neuromasts. **(G-N)** Individual slices of a neuromast following two regenerations at two different planes: apical hair cell layer (G-J) and basal support cell layer (K-N). EdU (visualized by a Click-iT reaction) is labeled in magenta, BrdU (anti-BrdU) is labeled in cyan, and myo6b:GFP hair cells are labeled in green. Arrowheads indicate EdU/BrdU-positive hair cells, and asterisks indicate EdU-positive support cells. Scale bar = 10 μm.

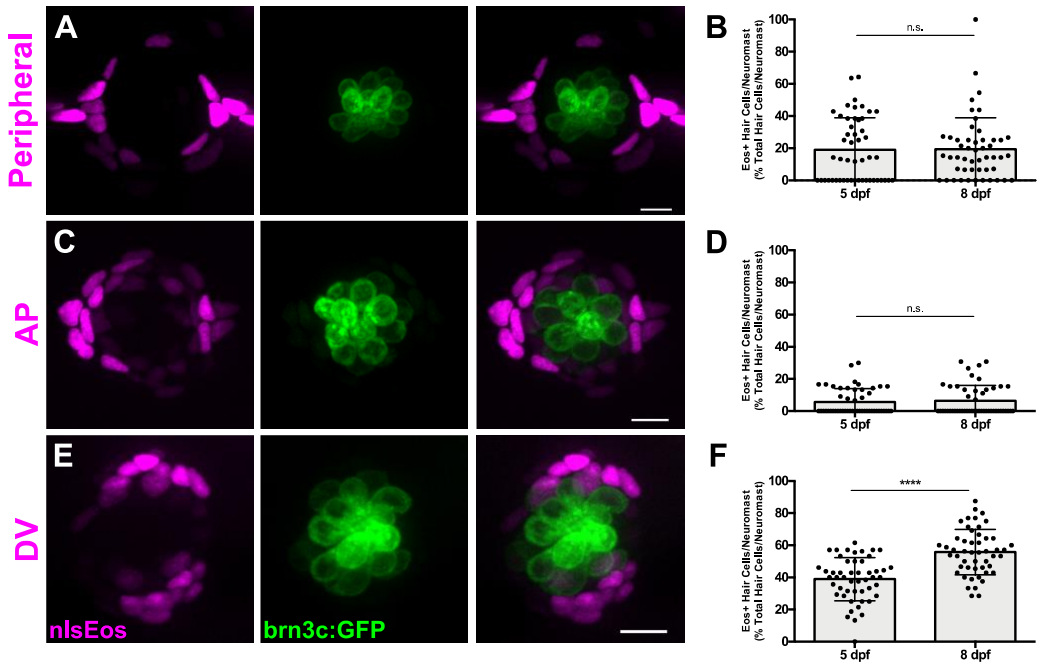

Figure 2.2. Genetic labeling of spatially-distinct support cell populations. **(A, C, E)** Maximum projections of neuromasts from *sfrp1a*:nlsEos (Peripheral, A), *tnfsf10l3*:nlsEos (AP, C), and *sost*:nlsEos (DV, E) fish. Converted nlsEos-positive cells are shown in magenta, and brn3c:GFP-positive hair cells are shown in green. Scale bar = 10 μm. **(B, D, F)** Percentage of hair cells per neuromast labeled by Peripheral (B), AP (D), and DV cells (F) at 5 and 8 dpf. **(B)** 5 dpf: 19.04 ± 19.86, n = 50 neuromasts; 8 dpf: 19.46 ± 19.44, n = 50 neuromasts; mean ± SD; Mann Whitney U test, p = 0.7047. **(D)** 5 dpf: 5.71 ± 8.22, n = 50 neuromasts; 8 dpf: 6.36 ± 9.57, n = 50 neuromasts; mean ± SD; Mann Whitney U test, p = 0.9668. **(F)** 5 dpf: 38.93 ± 13.46, n = 50 neuromasts; 8 dpf: 55.78 ± 14.13, n = 50 neuromasts; mean ± SD; Mann Whitney U test, p < 0.0001.

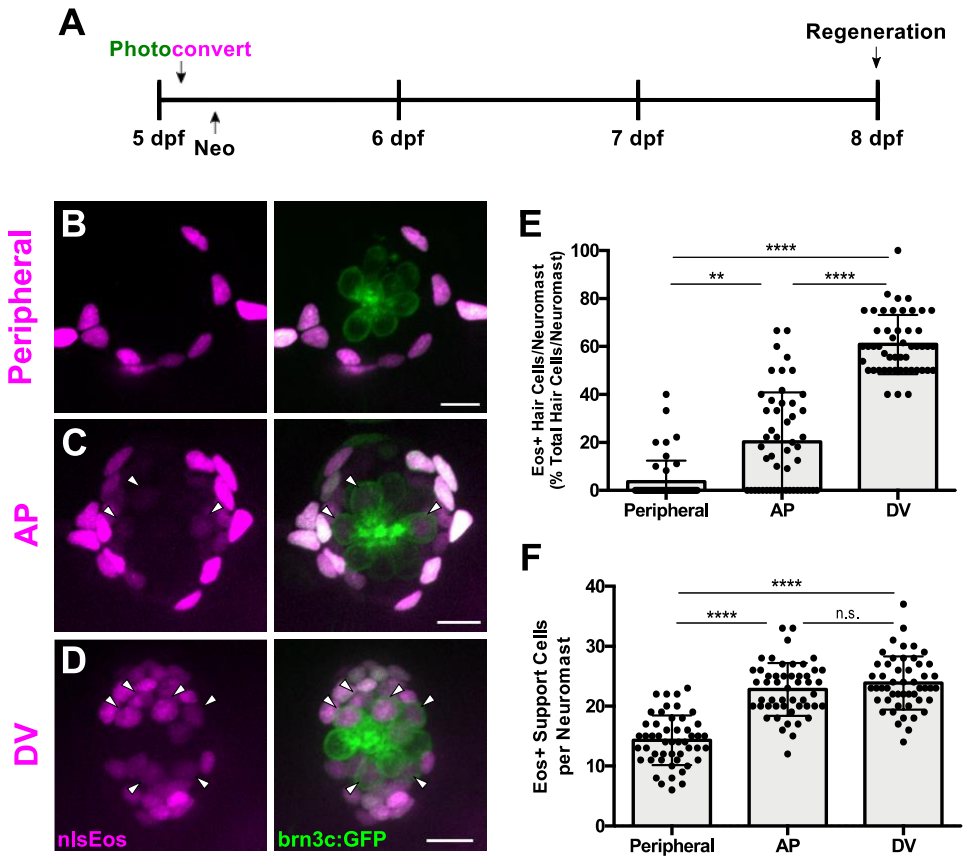

Figure 2.3. Distinct support cell populations have different regenerative capacities. **(A)** Timeline of nlsEos fate mapping experiment. Fish were photoconverted at 5 dpf, treated with neomycin, then fixed and imaged 72 hours post treatment (8 dpf). **(B, C, D)** Maximum projections of neuromasts from *sfrp1a*:nlsEos (Peripheral, B), *tnfsf10l3*:nlsEos (AP, C), and *sost*:nlsEos (DV, D) fish following photoconversion and hair cell regeneration. Converted nlsEos-positive cells are shown in magenta, and brn3c:GFP-positive hair cells are shown in green. Arrowheads indicate nlsEos-positive hair cells. Scale bar = 10 μm. **(E)** Percentage of hair cells per neuromast labeled by nlsEos following regeneration. *Sfrp1a*:nlsEos (Peripheral): 3.59 ± 8.87, n = 50 neuromasts; *tnfsf10l3*:nlsEos (AP): 20.28 ± 20.58, n = 50 neuromasts; *sost*:nlsEos (DV): 60.87 ± 12.37, n = 50 neuromasts; mean ± SD; Kruskal-Wallis test, Dunn's post-test, $p = 0.003$ (Peripheral vs. AP), $p < 0.0001$ (Peripheral vs. DV, AP vs. DV). **(F)** Total nlsEos-positive support cells per neuromast prior to hair cell ablation. *Sfrp1a*:nlsEos (Peripheral): 14.30 ± 4.17, n = 50 neuromasts; *tnfsf10l3*:nlsEos (AP): 22.8 ± 4.40, n = 50 neuromasts; *sost*:nlsEos (DV): 23.86 ± 4.45, n = 50 neuromasts; mean ± SD; Kruskal-Wallis test, Dunn's post-test, $p < 0.0001$ (Peripheral vs. AP, Peripheral vs. DV), $p > 0.9999$ (AP vs. DV).

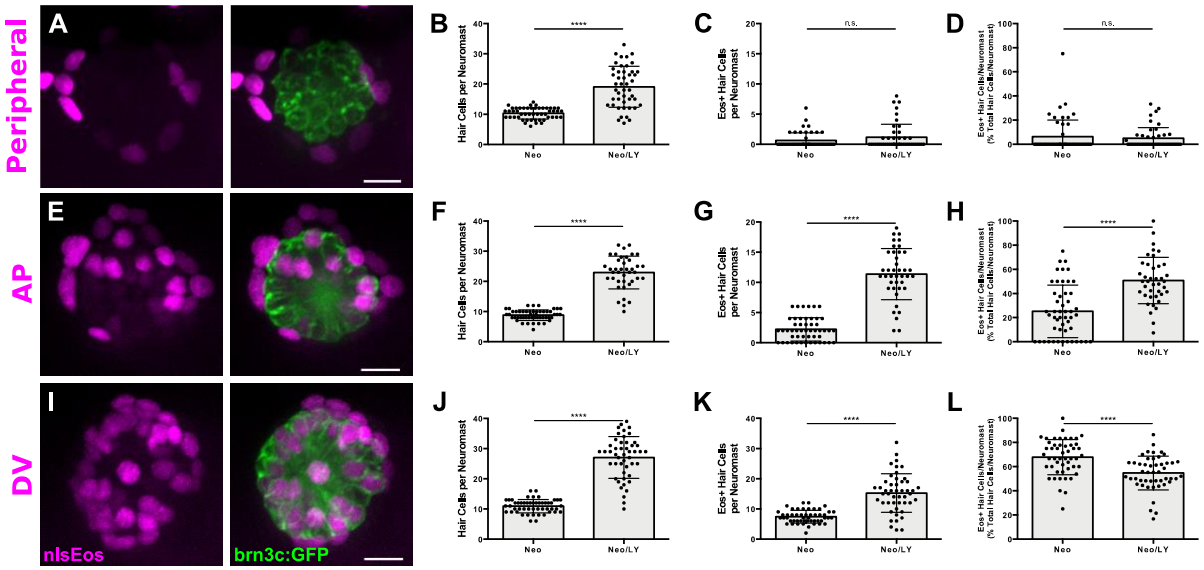

Figure 2.4. Notch signaling differentially regulates support cell populations. **(A, E, I)** Maximum projections of neuromasts expressing *sfrp1a*:nlsEos (Peripheral, A), *tnfsf10l3*:nlsEos (AP, E), and *sost*:nlsEos (DV, I) following Notch-inhibited hair cell regeneration. Converted nlsEos-positive cells are shown in magenta, and brn3c:GFP-positive hair cells are shown in green. Scale bar = 10 μm. **(B)** Total number of hair cells per neuromast in *sfrp1a*:nlsEos fish following hair cell regeneration. Neo: 10.28 ± 1.88, n = 50 neuromasts; Neo/LY: 19.07 ± 6.79, n = 46 neuromasts; mean ± SD; Mann Whitney U test, $p < 0.0001$. **(C)** *Sfrp1a*:nlsEos-positive hair cells per neuromast following hair cell regeneration. Neo: 0.62 ± 1.28, n = 50 neuromasts; Neo/LY: 1.15 ± 2.16, n = 46 neuromasts; mean ± SD; Mann Whitney U test, $p = 0.2481$. **(D)** Percentage of *sfrp1a*:nlsEos-labeled hair cells per neuromast following hair cell regeneration. Neo: 6.31 ± 13.83, n = 50 neuromasts; Neo/LY: 4.95 ± 8.82, n = 46 neuromasts; mean ± SD; Mann Whitney U test, $p = 0.5148$. **(F)** Total number of hair cells per neuromast in *tnfsf10l3*:nlsEos fish following hair cell regeneration. Neo: 8.84 ± 1.75, n = 50 neuromasts; Neo/LY: 22.93 ± 5.45, n = 40 neuromasts; mean ± SD; Mann Whitney U test, $p < 0.0001$. **(G)** *Tnfsf10l3*:nlsEos-positive hair cells per neuromast following hair cell regeneration. Neo: 2.22 ± 1.94, n = 50 neuromasts; Neo/LY: 11.38 ± 4.23, n = 40 neuromasts; mean ± SD; Mann Whitney U test, $p < 0.0001$. **(H)** Percentage of *tnfsf10l3*:nlsEos-labeled hair cells per neuromast following hair cell regeneration. Neo: 25.19 ± 21.72, n = 50 neuromasts; Neo/LY: 50.68 ± 19.23, n = 40 neuromasts; mean ± SD; Mann Whitney U test, $p < 0.0001$. **(J)** Total number of hair cells per neuromast in *sost*:nlsEos fish following hair cell regeneration. Neo: 10.94 ± 2.23, n = 50 neuromasts; Neo/LY: 27.06 ± 6.90, n = 48 neuromasts; mean ± SD; Mann Whitney U test, $p < 0.0001$. **(K)** *Sost*:nlsEos-positive hair cells per neuromast following hair cell regeneration. Neo: 7.40 ± 2.13, n = 50 neuromasts; Neo/LY: 15.25 ± 6.36, n = 48 neuromasts; mean ± SD; Mann Whitney U test, $p < 0.0001$. **(L)** Percentage of *sost*:nlsEos-labeled hair cells per neuromast following hair cell regeneration. Neo: 67.86 ± 14.63, n = 50 neuromasts; Neo/LY: 54.69 ± 14.01, n = 48 neuromasts; mean ± SD; Mann Whitney U test, $p < 0.0001$.

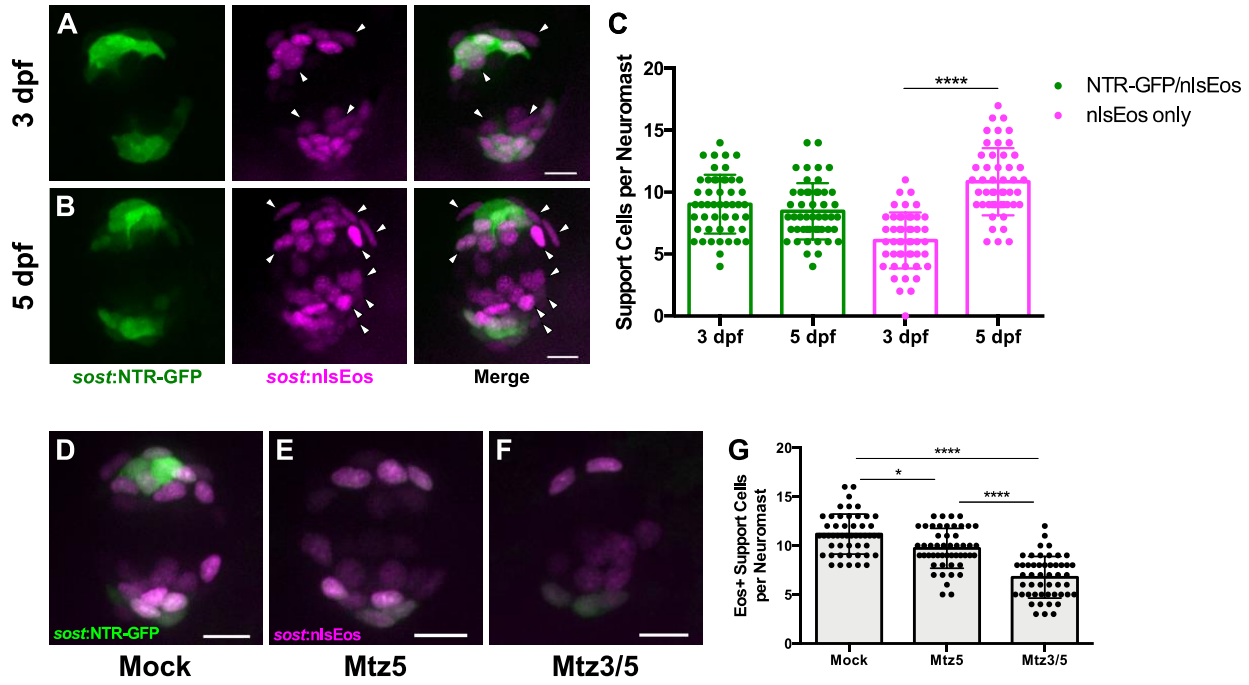

Figure 2.5. Differences in overlap between *sost*:NTR-GFP and *sost*:nlsEos populations. **(A-B)** Maximum projections of neuromasts from *sost*:NTR-GFP; *sost*:nlsEos fish at 3 dpf (A) and 5 dpf (B). *Sost*:NTR-GFP cells are shown in green and *sost*:nlsEos cells are shown in magenta. Arrowheads indicate cells expressing *sost*:nlsEos but not *sost*:NTR-GFP. Scale bar = 10 μm. **(C)** Support cells per neuromast expressing either NTR-GFP and nlsEos (green) or nlsEos only (magenta) at 3 dpf and 5 dpf. NTR-GFP/nlsEos: 9.04 ± 2.39 (3 dpf) vs. 8.47 ± 2.27 (5 dpf); n = 49 neuromasts; nlsEos only: 6.10 ± 2.27 (3 dpf) vs. 10.86 ± 2.72 (5 dpf); n = 49 neuromasts; mean ± SD; Kruskal-Wallis test, Dunn's post-test, $p > 0.9999$ (NTR-GFP/nlsEos 3 dpf vs. 5 dpf), $p < 0.0001$ (nlsEos only 3 dpf vs. 5 dpf). **(D-F)** Maximum projections of neuromasts from *sost*:NTR-GFP; *sost*:nlsEos fish following mock treatment (D; Mock), Mtz at 5 dpf (E; Mtz5), and Mtz at 3 dpf and 5 dpf (F; Mtz3/5). *Sost*:NTR-GFP cells are shown in green and *sost*:nlsEos cells are shown in magenta. Scale bar = 10 μm. **(G)** Support cells per neuromast solely expressing *sost*:nlsEos following Mtz treatment. Mock: 11.18 ± 2.04, n = 50 neuromasts; Mtz5: 9.72 ± 2.03, n = 50 neuromasts; Mtz3/5: 6.76 ± 2.12, n = 50 neuromasts; mean ± SD; Kruskal-Wallis test, Dunn's post-test, $p = 0.0288$ (Mock vs. Mtz5), $p < 0.0001$ (Mock vs. Mtz3/5, Mtz5 vs. Mtz3/5).

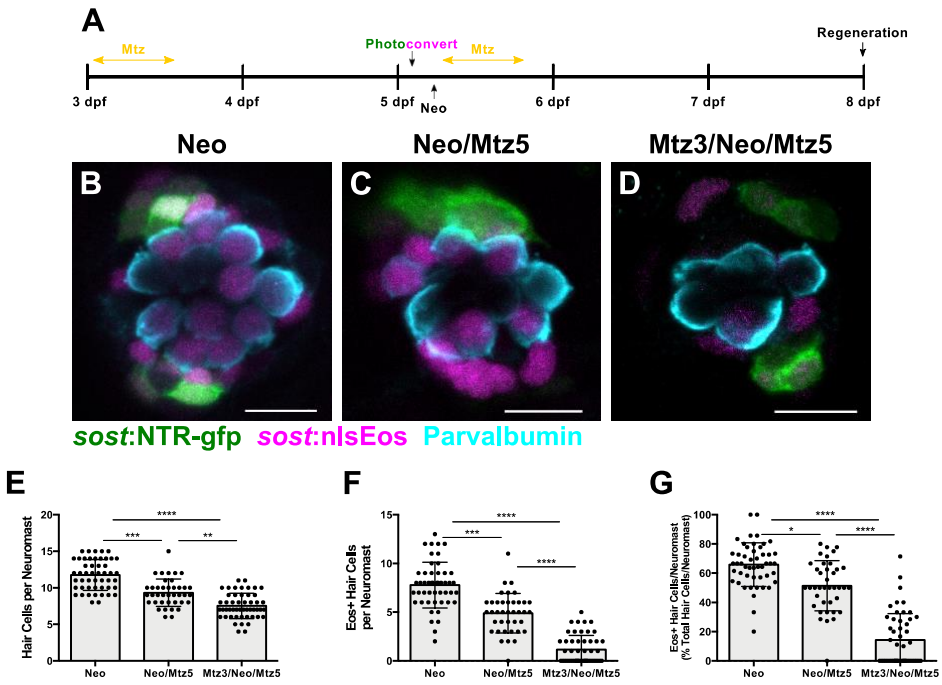

Figure 2.6. Ablation of DV cells decreases number of regenerated hair cells. **(A)** Timeline of DV cell-ablation experiment. Larvae were treated with Mtz at 3 dpf, photoconverted, then treated with neomycin, then treated with Mtz again at 5 dpf, and fixed and immunostained at 72 hpt (8 dpf). **(B-D)** Maximum projections of neuromasts from *sost*:NTR-GFP; *sost*:nlsEos fish following neomycin (B; Neo), neomycin and Mtz (C; Neo/Mtz5), and Mtz, neomycin, and Mtz treatments (D; Mtz3/Neo/Mtz5). *Sost*:NTR-GFP cells are shown in green, *sost*:nlsEos cells are shown in magenta, and anti-Parvalbumin-stained hair cells are shown in cyan. Scale bar = 10 μm. **(E)** Total hair cells per neuromast following regeneration. Neo: 11.73 ± 2.10, n = 49 neuromasts; Neo/Mtz5: 9.33 ± 1.88, n = 39 neuromasts; Mtz3/Neo/Mtz5: 7.52 ± 1.74, n = 50 neuromasts; mean ± SD; Kruskal-Wallis test, Dunn's post-test, p = 0.0001 (Neo vs. Neo/Mtz5), p < 0.0001 (Neo vs. Mtz3/Neo/Mtz5), p = 0.0016 (Neo/Mtz5 vs. Mtz3/Neo/Mtz5). **(F)** *Sost*:nlsEos-positive hair cells per neuromast following regeneration. Neo: 7.78 ± 2.36, n = 49 neuromasts; Neo/Mtz5: 4.90 ± 2.02, n = 39 neuromasts; Mtz3/Neo/Mtz5: 1.16 ± 1.46, n = 50 neuromasts; mean ± SD; Kruskal-Wallis test, Dunn's post-test, p = 0.0003 (Neo vs. Neo/Mtz5), p < 0.0001 (Neo vs. Mtz3/Neo/Mtz5, Neo/Mtz5 vs. Mtz3/Neo/Mtz5). **(G)** Percentage of hair cells per neuromast labeled by *sost*:nlsEos following regeneration. Neo: 65.81 ± 14.89, n = 49 neuromasts; Neo/Mtz5: 51.40 ± 17.17, n = 39 neuromasts; Mtz3/Neo/Mtz5: 14.29 ± 18.10, n = 50 neuromasts; mean ± SD; Kruskal-Wallis test, Dunn's post-test, p = 0.0147 (Neo vs. Neo/Mtz5), p < 0.0001 (Neo vs. Mtz3/Neo/Mtz5, Neo/Mtz5 vs. Mtz3/Neo/Mtz5).

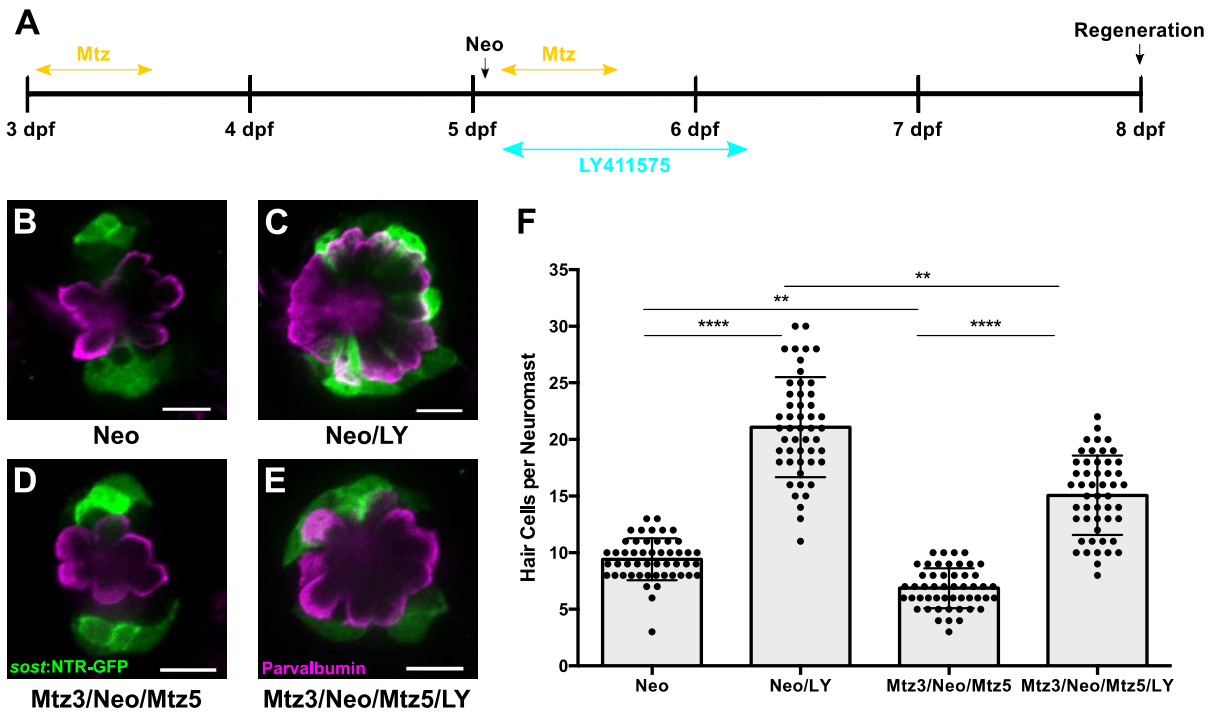

Figure 2.7. DV cell-ablation reduces the number of supernumerary hair cells formed during Notch-inhibited hair cell regeneration. **(A)** Timeline of dual DV cell-ablation, Notch-inhibition experiment. *Sost*:NTR-GFP larvae were treated with Mtz at 3 dpf, treated with neomycin at 5dpf, then co-treated with Mtz and LY411575 for 8 hours, then washed out and treated with LY411575 for 16 additional hours (24 hours total LY). **(B-E)** Maximum projections of *sost*:NTR-GFP neuromasts following normal hair cell regeneration (B; Neo), Notch-inhibited hair cell regeneration (C; Neo/LY), DV cell-ablated hair cell regeneration (D; Mtz3/Neo/Mtz5), and DV cell-ablated and Notch-inhibited hair cell regeneration (E; Mtz3/Neo/Mtz5/LY). *Sost*:NTR-GFP cells are shown in green, and anti-Parvalbumin immunostained hair cells are shown in magenta. Scale bar = 10 μm. **(F)** Total number of hair cells per neuromast following hair cell regeneration. Neo: 9.42 ± 1.85, n = 50 neuromasts; Neo/LY: 21.08 ± 4.42, n = 50 neuromasts; Mtz3/Neo/Mtz5: 6.86 ± 1.76, n = 50 neuromasts; Mtz3/Neo/Mtz5/LY: 15.06 ± 3.51, n = 50 neuromasts; mean ± SD; Kruskal-Wallis test, Dunn's post-test, $p < 0.0001$ (Neo vs. Neo/LY; Mtz3/Neo/Mtz5 vs. Mtz3/Neo/Mtz5/LY), $p = 0.0058$ (Neo vs. Mtz3/Neo/Mtz5), $p = 0.0029$ (Neo/LY vs. Mtz3/Neo/Mtz5/LY).

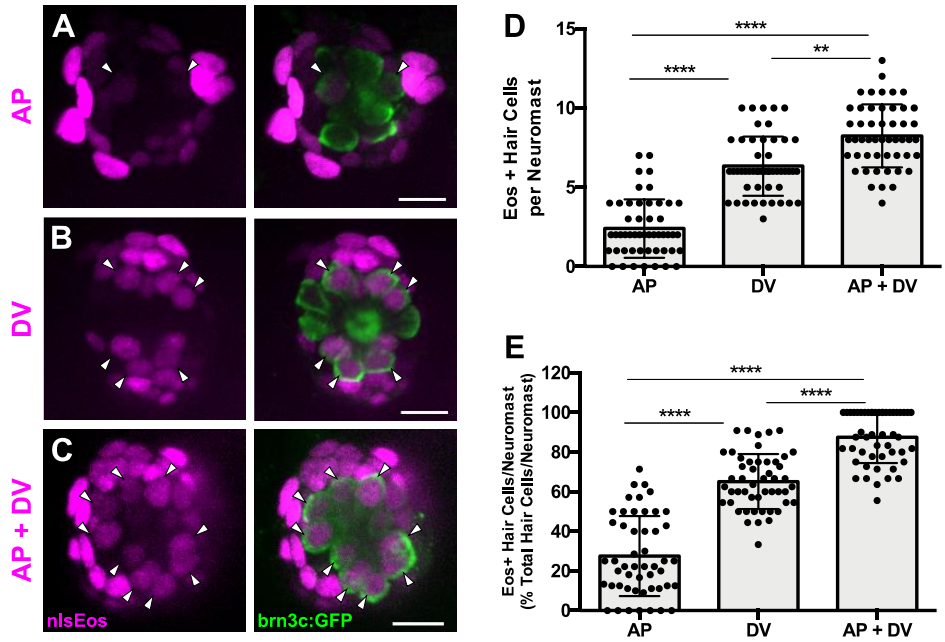

Figure 2.8. AP cells and DV cells define distinct progenitor populations. **(A-C)** Maximum projections of neuromasts from *tnfsf10l3*:nlsEos (AP, A), *sost*:nlsEos (DV, B), and *tnfsf10l3*:nlsEos/*sost*:nlsEos fish (AP + DV, C) following photoconversion and regeneration. Converted nlsEos-positive cells are shown in magenta, and brn3c:GFP-positive hair cells are shown in green. Arrowheads indicate nlsEos-positive hair cells. Scale bar = 10 μm. **(D)** Number of nlsEos-positive hair cells per neuromast in each of the nlsEos lines following regeneration. *Tnfsf10l3*:nlsEos (AP): 2.4 ± 1.84, n = 50 neuromasts; *sost*:nlsEos (DV): 6.34 ± 1.87, n = 50 neuromasts; *tnfsf10l3*:nlsEos/*sost*:nlsEos (AP + DV): 8.24 ± 1.99, n = 50 neuromasts; mean ± SD; Kruskal-Wallis test, Dunn's post-test, $p < 0.0001$ (AP vs. DV, AP vs. AP + DV), $p = 0.0031$ (DV vs. AP + DV). **(E)** Percentage of hair cells per neuromast labeled by nlsEos lines following regeneration. AP: 27.59 ± 20.21, n = 50 neuromasts; DV: 65.16 ± 13.89, n = 50 neuromasts; AP + DV: 87.57 ± 13.02, n = 50 neuromasts; mean ± SD; Kruskal-Wallis test, Dunn's post-test, $p < 0.0001$ (all comparisons).

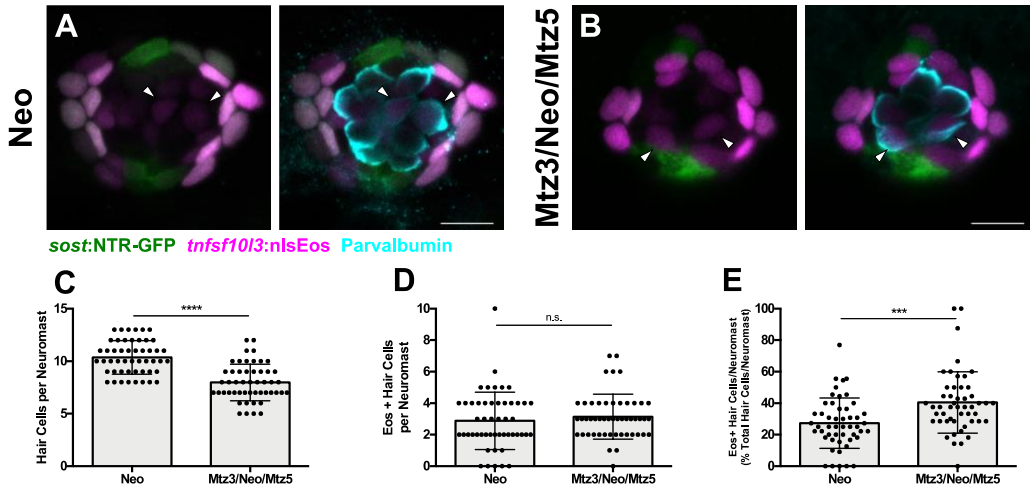

Figure 2.9. AP population doesn't compensate for the loss of the DV population during hair cell regeneration. **(A-B)** Maximum projections of *tnfsf10l3*:nlsEos; *sost*:NTR-GFP neuromasts following normal hair cell regeneration (A; Neo) or DV cell-ablated hair cell regeneration (B; Mtz3/Neo/Mtz5). *Sost*:NTR-GFP cells are shown in green, *tnfsf10l3*:nlsEos cells are shown in magenta, and anti-Parvalbumin-stained hair cells are shown in cyan. Arrowheads indicate nlsEos-positive hair cells. Scale bar = 10 μm. **(C)** Total number of hair cells per neuromast following hair cell regeneration. Neo: 10.36 ± 1.60, n = 50 neuromasts; Mtz3/Neo/Mtz5: 7.98 ± 1.74, n = 50 neuromasts; mean ± SD; Mann Whitney U test, $p < 0.0001$. **(D)** Number of nlsEos-positive hair cells per neuromast following hair cell regeneration. Neo: 2.88 ± 1.83, n = 50 neuromasts; Mtz3/Neo/Mtz5: 3.14 ± 1.43, n = 50 neuromasts; mean ± SD; Mann Whitney U test, $p = 0.3855$. **(E)** Percentage of hair cells per neuromast labeled by nlsEos following hair cell regeneration. Neo: 27.26 ± 16.00, n = 50 neuromasts; Mtz3/Neo/Mtz5: 40.43 ± 19.44, n = 50 neuromasts; mean ± SD; Mann Whitney U test, $p = 0.0002$.

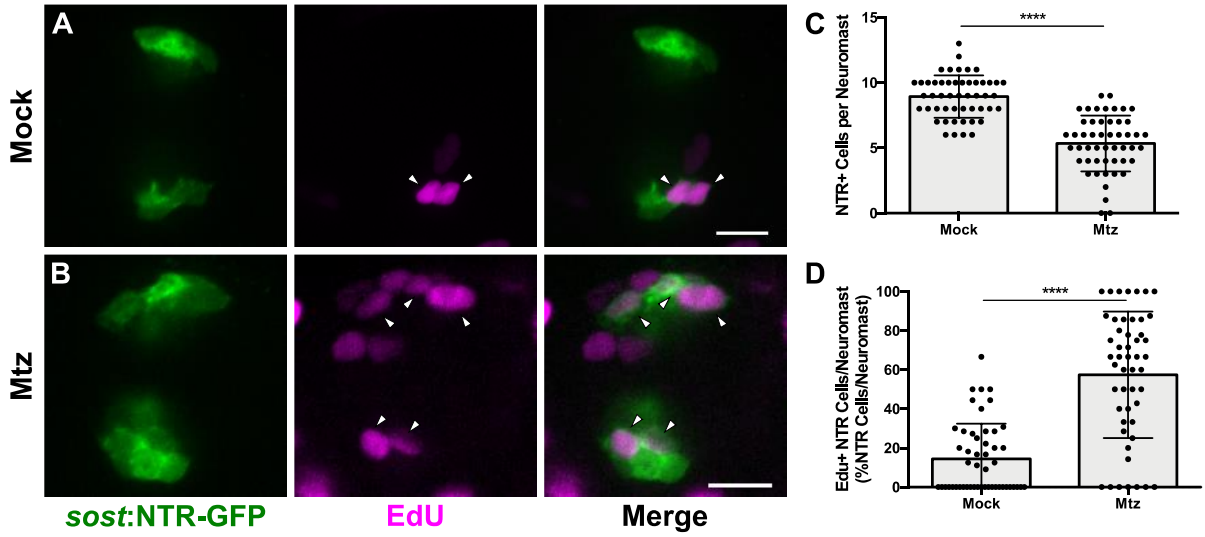

Figure 2.10. DV population regenerates via proliferation. **(A-B)** Maximum projections of neuromasts from *sost*:NTR-GFP fish either untreated (A; Mock) or treated with 10 mM Mtz (B; Mtz). *Sost*:NTR-GFP cells are shown in green and EdU-positive cells are shown in magenta. Arrowheads indicate EdU-positive *sost*:NTR-GFP cells. Scale bar = 10 μm. **(C)** Total number of *sost*:NTR-GFP cells per neuromast following DV cell regeneration. Mock: 8.94 ± 1.62, n = 50 neuromasts; Mtz: 5.34 ± 2.14, n = 50 neuromasts; mean ± SD; Mann Whitney U test, $p < 0.0001$. **(D)** Percentage of *sost*:NTR-GFP cells per neuromast labeled by EdU following DV cell regeneration. Mock: 14.47 ± 17.95, n = 50 neuromasts; Mtz: 57.49 ± 32.34, n = 50 neuromasts; mean ± SD; Mann Whitney U test, $p < 0.0001$.

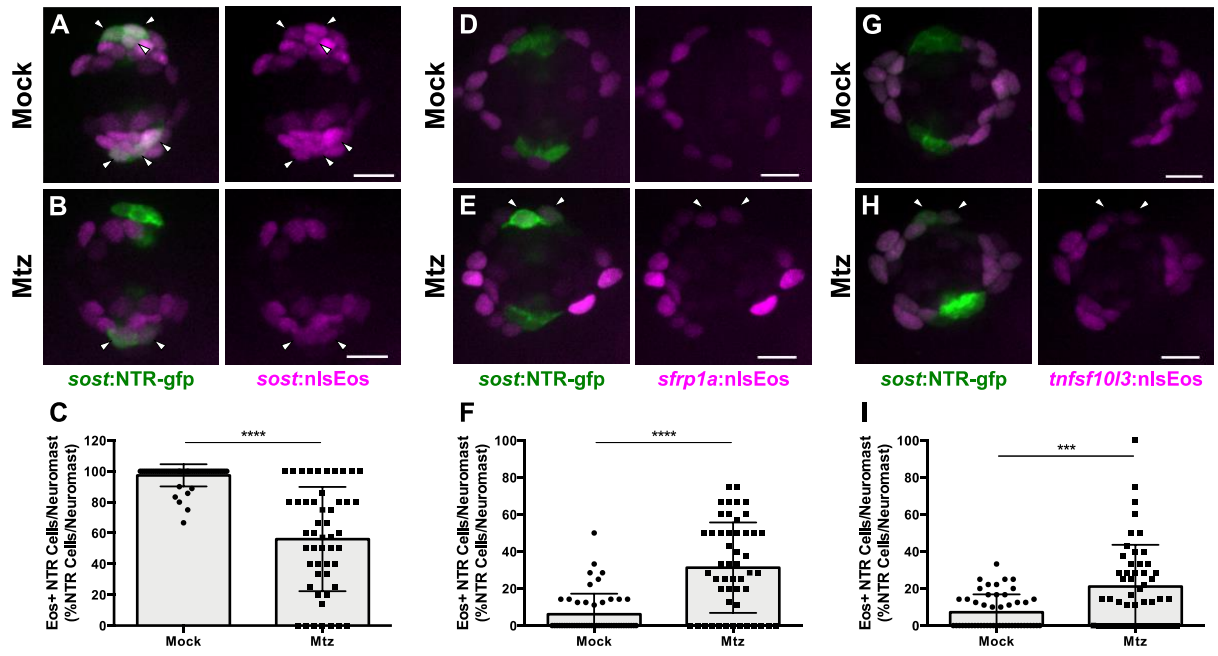

Figure 2.11. DV cells are replenished by other support cell populations. **(A-B, D-E, G-H)** Maximum projections of neuromasts expressing *sost*:NTR-GFP and *sost*:nlsEos (A-B), *sfrp1a*:nlsEos (D-E), and *tnfsf10l3*:nlsEos (G-H) in the absence of (A, D, G; Mock) or following Mtz-induced DV cell ablation (B, E, H; Mtz). *Sost*:NTR-GFP cells are shown in green and nlsEos-positive cells are shown in magenta. Arrowheads indicate nlsEos-positive *sost*:NTR-GFP cells. Scale bar = 10 μm. **(C)** Percentage of *sost*:NTR-GFP cells per neuromast labeled by *sost*:nlsEos following DV cell regeneration. Mock: 97.39 ± 7.14, n = 50 neuromasts; Mtz: 56.09 ± 33.72, n = 50 neuromasts; mean ± SD; Mann Whitney U test, $p < 0.0001$. **(F)** Percentage of *sost*:NTR-GFP cells per neuromast labeled by *sfrp1a*:nlsEos following DV cell regeneration. Mock: 6.15 ± 11.14, n = 50 neuromasts; Mtz: 31.27 ± 24.41, n = 50 neuromasts; mean ± SD; Mann Whitney U test, $p < 0.0001$. **(I)** Percentage of *sost*:NTR-GFP cells per neuromast labeled by *tnfsf10l3*:nlsEos following DV cell regeneration. Mock: 7.31 ± 9.55, n = 50 neuromasts; Mtz: 21.11 ± 22.51, n = 50 neuromasts; mean ± SD; Mann Whitney U test, $p = 0.0004$.

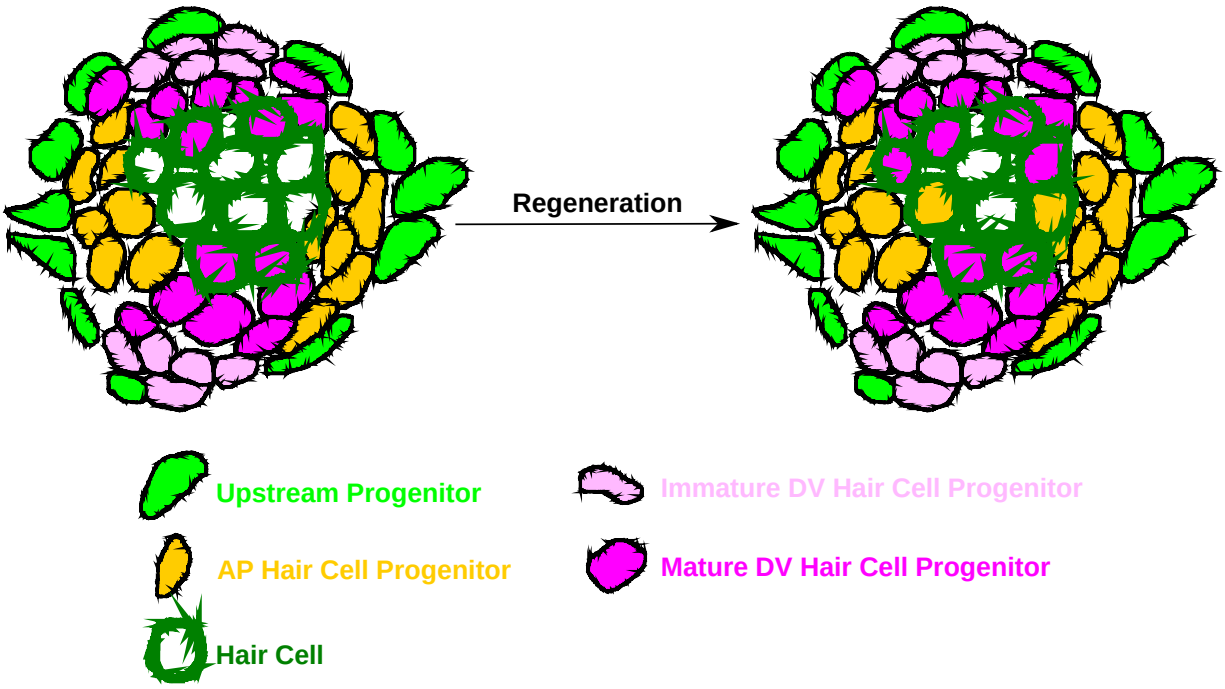

Figure 2.12. Model of neuromast progenitor identity. *Sost*:nlsEos-positive cells, located in the dorsoventral (DV) region of the neuromast, contain immature hair cell progenitors (shown in light pink) and mature hair cell progenitors (shown in magenta). Immature hair cell progenitors do not directly generate new hair cells (outlined in dark green) during regeneration, but do become mature hair cell progenitors, which comprise the majority of hair cell progenitors (see magenta-filled hair cells following regeneration). *Tnfsf10l3*:nlsEos-positive cells (shown in gold), located in the anteroposterior (AP) region of the neuromast, also serve as hair cell progenitors (see gold-filled hair cells following regeneration). Both of these populations are regulated by Notch signaling, and both can replenish immature hair cell progenitors. Finally, *sfrp1a*:nlsEos-positive cells (shown in light green), located in the periphery, do not serve as hair cell progenitors, nor are they regulated by Notch signaling. However, they are capable of replenishing immature hair cell progenitors, and can thus be classified as an upstream progenitor.

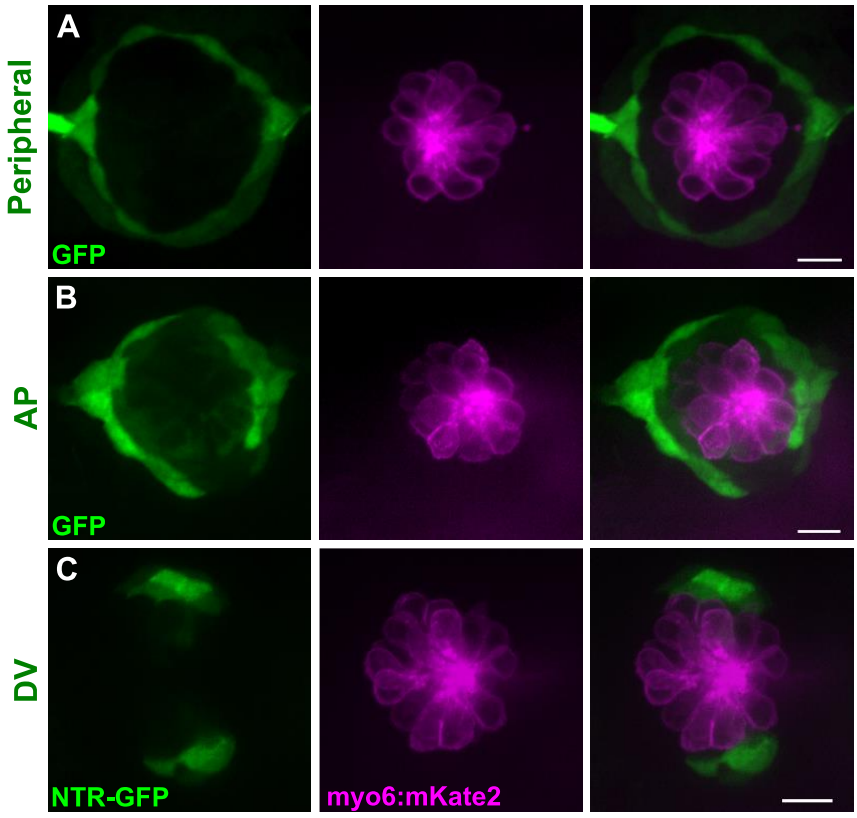

Supplemental Figure 2.13. Support cell transgenes are not expressed in hair cells. **(A-C)** Maximum projections of neuromasts from Tg[*sfrp1a*:GFP]^{w222} (Peripheral, A), Tg[*tnfsf10l3*:GFP]^{w223} (AV, B), and *sost*:NTR-GFP (DV, C) fish. GFP-positive cells are shown in green, and hair cells are shown in magenta via myo6:mKate2. In all three populations, there is no GFP expression in hair cells. Scale bar = 10 μm.

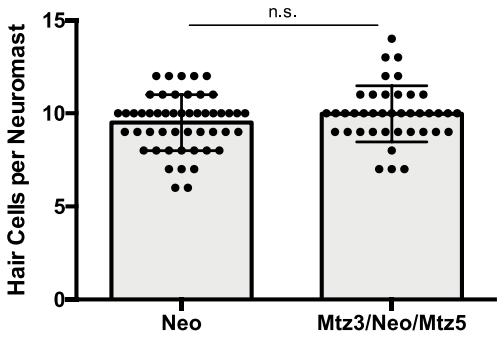

Supplemental Figure 2.14. Mtz treatment does not inherently impact hair cell regeneration. Total number of hair cells per neuromast following regular hair cell regeneration (Neo) or DV cell-ablated regeneration (Mtz3/Neo/Mtz5) in non-transgenic siblings of *sost*:NTR-GFP fish. Neo: 9.5 ± 1.50, n = 50 neuromasts; Mtz3/Neo/Mtz5: 9.98 ± 1.51, n = 40 neuromasts; mean ± SD; Mann Whitney U test, p = 0.2317.

CHAPTER 3

REGENERATION IN THE ZEBRAFISH INNER EAR IS MEDIATED BY TRANSDIFFERENTIATION

3.1 Introduction

The zebrafish lateral line has long been a model for the regeneration of mechanosensory hair cells. The sensory organs of the lateral line, the neuromasts, are located on the surface of the body, allowing for easy visualization as well experimental manipulation. Following hair cell death, new hair cells arise from the symmetric division of the surrounding support cells (I. A. Cruz et al., 2015; López-Schier & Hudspeth, 2006; Ma et al., 2008; Romero-Carvajal et al., 2015; Wibowo et al., 2011). These progenitor cells are also replenished by other support cells (see Chapter 2). However, zebrafish also have an inner ear, which is comprised of a number of sensory epithelia, including the three cristae, the saccule, the utricle, and the lagena. While the other organs are fully developed and functional in larval zebrafish, the lagena doesn't fully develop until the juvenile stage (Bever & Fekete, 2002; Nicolson, 2005; Vanwalleghem et al., 2017). As a result of the accessibility of the lateral line, there have been few studies on inner ear regeneration in zebrafish. One study by Schuck and Smith 2009 found that saccular hair cells were capable of regenerating following noise-induced damage in adult zebrafish, but were unable to determine whether this regeneration occurred via transdifferentiation or proliferation. In another study, hair cells in the larval utricle were capable of regenerating after laser ablation, and this regeneration was mediated by transdifferentiation of surrounding support cells (Millimaki et al., 2010). In this study, we have generated a novel transgenic line in which hair cells, including those of the inner ear, are genetically-targeted for cell-specific ablation. We

demonstrate that, following ablation, hair cells of the larval cristae are capable of regeneration and that this regeneration is primarily mediated via transdifferentiation.

3.2 Results

3.2.1 Hair Cells Expressing Mammalian TrpV1 Channels Can be Selectively Ablated with Capsaicin

In order to be able to successfully ablate inner ear hair cells, we needed a compound that could permeate into the inner ear and selectively damage hair cells, something that aminoglycoside antibiotics are unable to do. Rather than rely on any drugs, we turned to the mammalian TrpV1 system pioneered by Chen et al. 2016. Unlike mammalian TrpV1 channels, zebrafish TrpV1 channels do not respond to capsaicin (Gau et al., 2013), and thus capsaicin can be used to drive activity in or to ablate (depending on the concentration) zebrafish cells that express the mammalian receptor. We thus sought to drive the expression of mammalian TrpV1 channels in zebrafish hair cells. To this end, we generated a Tol2 construct in which rat TrpV1 (rTrpV1) and the GFP-variant mClover were bicistronically expressed under the myosin6b promoter (myo6b:rTrpV1-e2a-mClover) and injected it into wildtype embryos. Larvae were screened for mClover expression at 3 dpf and then incubated in the red vital dye FM 4-64 to label all lateral line hair cells. Figure 3.1A shows an example of an anterior neuromast transiently expressing mClover in a subset of hair cells. Larvae were then incubated in 10 μM capsaicin for one hour, which was sufficient to ablate all mClover-expressing hair cells. Figure 3.1B shows the same neuromast after capsaicin treatment, and only the hair cells solely expressing FM 4-64 remain, indicating that capsaicin treatment does not affect hair cells not expressing rTrpV1. We thus concluded that we could use mammalian TrpV1 expression to selectively ablate hair cells in zebrafish.

3.2.2 Inner Ear Hair Cells Regenerate After Ablation

It was difficult to test ablation of inner ear hair cells in F_0 larvae, so we generated the stable line Tg[myo6b:rTrpV1-e2a-mClover]^{w221}, hereafter known as myo6:rTrpV1). In these fish, rTrpV1 is expressed throughout the cristae and maculae of the inner ear in addition to the lateral line. We found that treating 3 dpf larvae with 10 μM capsaicin for one hour was sufficient to ablate all hair cells in the inner ear and lateral line. Furthermore, larvae demonstrated notable vestibular defects for a day or so following treatment, indicating loss of inner ear function (data not shown). Having established a paradigm for inner ear hair cell ablation, we next examined whether inner ear hair cells were capable of regeneration. 5 dpf larvae were treated with capsaicin and fixed and immunostained for GFP at 24, 48, and 72 hours post treatment (hpt) (Fig. 3.2C-E). Larvae were also fixed and stained prior to treatment, immediately after treatment, and in the absence of treatment at 72 hpt (Fig. 3.2A, B, F). Due to their more superficial location, we focused our analysis on the three cristae of the inner ear. As expected, following capsaicin treatment, all hair cells in the cristae were gone (Fig. 3.2G; 0 ± 0). At 24 hpt, there were nearly 10 hair cells per crista, and this number significantly increased to 12 hair cells per crista at 48 hpt (9.53 ± 2.02 vs. 11.87 ± 2.49, $p = 0.0085$). However, there was no significant difference in hair cell number between 48 hpt and 72 hpt (11.87 ± 2.49 vs. 11.65 ± 2.61, $p > 0.9999$). Even after three days, there were still significantly fewer hair cells per crista compared to unablated fish (11.65 ± 2.61 vs. 17.35 ± 2.86 [72 hpt vs. Pre-Tx], 11.65 ± 2.61 vs. 17.57 ± 2.27 [72 hpt vs. Mock], $p < 0.0001$). However, it must be noted that proper vestibular function seemed to be restored after 48 hpt. Importantly, there was no difference in hair cell number between cristae prior to capsaicin treatment and mock-treated larvae (17.35 ± 2.86 vs. 17.57 ± 2.27), indicating

that this increase in hair cell number was not due to developmental addition. It must be noted that we did observe significantly more hair cells in the lateral crista compared to the anterior and posterior cristae, but the general trend in regeneration remained the same across epithelia (data not shown). Based on these data, we can conclude that inner ear hair cells are capable of regenerating.

3.2.3 Inner Ear Hair Cell Regeneration Occurs Primarily Via Transdifferentiation

We next sought to determine whether inner ear hair cells regenerated via proliferation, as they do in the lateral line. Since lateral line support cell proliferation occurs within the first 24 hours after hair cell damage (Ma et al., 2008), we incubated myo6:rTrpV1 larvae in EdU for 24 hours following capsaicin treatment. However, despite the fact that the majority of hair cells regenerated in the first 24 hours (Fig. 3.2G), we saw very few EdU-positive hair cells (data not shown). We thus decided to administer EdU pulses in 24-hour intervals following capsaicin-mediated hair cell death in case there was any late stage proliferative regeneration. Following capsaicin treatment at 5 dpf, myo6:rTrpV1 larvae were incubated in EdU from 0-24 hpt, 24-48 hpt, or 48-72 hpt, then fixed and immunostained at 72 hpt. As in the previous experiment, there was very little proliferation in the first 24 hours of regeneration, with only 3% of regenerated hair cells being EdU-positive (Fig. 3.3A, E; 3.11 ± 4.76). However, we observed absolutely no proliferation after the other two 24-hour EdU intervals (Fig. 3.3B-C, E), indicating that hair cell regeneration within the inner ear is predominately mediated by transdifferentiation as opposed to proliferation.

3.3 Discussion

The regeneration of inner ear hair cells via transdifferentiation stands in stark contrast with regeneration in the lateral line, which occurs via proliferation (I. A. Cruz et al., 2015; López-Schier & Hudspeth, 2006; Ma et al., 2008; Romero-Carvajal et al., 2015; Wibowo et al., 2011). While transdifferentiation cannot be completely ruled out, blocking proliferation after hair cell death prevents formation of any new hair cells (Mackenzie & Raible, 2012). However, the mechanism of transdifferentiation is observed in a number of other species. In the avian auditory epithelium, regenerated hair cells initially arise via transdifferentiation of support cells, with later addition occurring via proliferation (Corwin & Cotanche, 1988; David W. Roberson et al., 2004). Blocking proliferation reduces the number of regenerated hair cells, but does not interfere with early transdifferentiation (Adler & Raphael, 1996; Shang et al., 2010). This combination of proliferation and transdifferentiation has also been observed in the bullfrog inner ear (Baird, Burton, Fashena, Naeger, & Naeger, 2000; Baird, Steyger, & Schuff, 1996). Transdifferentiation has also been observed, albeit in a limited fashion, in the mammalian utricle and cristae (Bucks et al., 2017; Slowik & Bermingham-McDonogh, 2013). The timing of these non-mitotic and mitotic events is the opposite of what we observed in the zebrafish inner ear, with proliferation occurring early in the regenerative process rather than later. However, the number of regenerated hair cells did not return to control levels at 72 hpt, so it could be that complete regeneration takes longer than three days in the inner ear. If so, perhaps later regeneration events could occur via proliferation. It will also be important to perform these experiments in the presence of mitotic inhibitors to examine if proliferation is truly dispensable for inner ear hair cell regeneration. Finally, since inhibition of Notch signaling results in an increase in regenerated hair cells in both the zebrafish lateral line (Ma et al., 2008; Romero-Carvajal et al., 2015; Wibowo et al., 2011)

and the mammalian inner ear (Mizutari et al., 2013; Slowik & Bermingham-McDonogh, 2013), it is possible that inhibiting Notch following capsaicin-mediated ablation could increase the number of regenerated hair cells in the zebrafish inner ear.

It is also important to note that we only assayed hair cell regeneration in the cristae; these experiments will need to be repeated in the utricle and saccule as well. Consistent with our findings, a previous study showed that transdifferentiation mediates regeneration in the larval utricle (Millimaki et al., 2010). However, these experiments were performed at 30 hpf, a stage at which inner ear epithelia are still developing. Furthermore, only a subset of utricular hair cells were targeted for laser ablation, and BrdU was only administered for a period of three hours. While it could very well be true that utricular hair cells predominantly regenerate via transdifferentiation, our novel rTrpV1 line would provide a more robust tool for examining utricular regeneration. The same holds true for the larval saccule. In addition, whether these mechanisms of regeneration persist into adulthood will also need to be examined. One study has shown that hair cells in the adult saccule regenerate after noise-induced damage (Schuck & Smith, 2009). The authors observed a significant increase in BrdU-positive cells following damage, but were not able to examine whether this BrdU-labeling colocalized with hair cell bodies. It is thus unclear whether the regenerated hair cells arose from proliferation or transdifferentiation. Again, we can use our rTrpV1 line to examine hair cell regeneration in the adult inner ear.

Finally, although we have shown that hair cells in the larval crista regenerate, we do not yet know if this regeneration is accompanied by a restoration of inner ear function. Following capsaicin-treatment, larvae were incapable of remaining upright while swimming and spent a lot of time laying on their sides, behavior that is indicative of inner ear disfunction. However, they

regained their proper swimming behavior within two days of treatment. This observation leads us to believe that inner ear function has been restored by this time, but there are more robust and quantitative means to test larval inner ear function, such as the acoustic startle response or prepulse inhibition assay (Bhandiwad, Raible, Rubel, & Sisneros, 2018; Bhandiwad, Zeddies, Raible, Rubel, & Sisneros, 2013). These assays could be performed prior to capsaicin treatment and after regeneration to better establish whether this hair cell regeneration leads to restoration of inner ear function.

That transdifferentiation may be the primary mechanism of hair cell regeneration in the inner ear raises questions about the long-term regenerative capacity of the inner ear. In the lateral line, progenitor cells divide symmetrically to form two daughter hair cells (López-Schier & Hudspeth, 2006; Wibowo et al., 2011). While this could theoretically lead to depletion of the progenitor pool over time, the regenerative capacity of lateral line neuromasts is not diminished after successive hair cell ablation (I. A. Cruz et al., 2015; Pinto-Teixeira et al., 2015), indicating that these progenitors are also replenished. In fact, our work described in Chapter 2 provides concrete evidence of progenitor replacement. It remains unknown whether the support cells of the inner ear are replenished following their transdifferentiation into hair cells. If these progenitors are not replaced, then the long-term regenerative capacity of the inner ear would be limited. While the increase in BrdU-labeled cells in the adult saccule following noise damage suggests replacement of the surrounding support cells (Schuck & Smith, 2009), we could test the regenerative capacity of the inner ear by subjecting the rTrpV1 fish to successive ablations and examining the regenerative response. If the inner ear progenitors transdifferentiate without replacement, then regeneration should decrease after multiple capasaicin treatments.

3.4 Materials and Methods

Fish Maintenance

Experiments were conducted on 5-8 dpf larval zebrafish. Larvae were raised in E3 embryo medium (14.97 mM NaCl, 500 μM KCL, 42 μM Na_2HPO_4, 150 μM KH_2PO_4, 1 mM $CaCl_2$ dihydrate, 1 mM $MgSO_4$, 0.714 mM $NaHCO_3$, pH 7.2) at 28.5°C. All wildtype animals were of the AB strain. Zebrafish experiments and husbandry followed standard protocols in accordance with University of Washington Institutional Animal Care and Use Committee guidelines.

Plasmid Construction

The myo6b:rTrpV1-e2a-mClover construct was generated via the Gateway Tol2 system (Invitrogen). A pME-rTrpV1 (the rat TrpV1 coding sequence was cloned from a vector provided by Ajay Dhaka) construct and a p3E-e2a-mClover construct were generated via BP recombination, and then a pDEST-myo6b:rTrpV1-e2a-mClover construct was generated via LR recombination of p5E-myo6b, pME-rTrpV1, p3E-e2a-mClover, and pDEST-iTol2-pA2 vectors. All plasmids were maxi prepped (Qiagen) prior to injection.

Tol2 Transgenesis

The Tg(myo6b:rTrpV1-e2a-mClover)^{w221} line (hereafter known as myo6:rTrpV1) was generated via Tol2 transgenesis. 1-2 nL of a 5 μL injection mix consisting of 20 ng/μL myo6b:rTrpV1-e2a-mClover plasmid, 40 ng/μL transposase mRNA, and 0.2% phenol red were injected into single cell wildtype embryos. Larvae were screened for expression at 3 dpf and transgenic F_0 larvae were grown to adulthood. F_0 adults were outcrossed to wildtype fish, transgenic offspring were once again grown to adulthood, and the resulting adults were used to maintain a stable line.

Capsaicin Treatment

In order to ablate inner ear hair cells, larvae were incubated in 10 μM capsaicin (Sigma #M2028; 0.01% DMSO) in E3 medium for one hour in 60 x 15 mm petri dishes, then washed with fresh E3 medium three times. Capsaicin was stored at -80°C in 100 mM aliquots in DMSO.

EdU Treatment

Following hair cell ablation with capsaicin, larvae were incubated in 500 μM F-ara-EdU (Sigma #T511293) in E3 medium for 24 hours, then washed three times with fresh E3 medium. F-ara-EdU was originally reconstituted in 50% H_2O and 50% DMSO to 50 mM, so the working concentration of DMSO of 500 μM was 0.5%.

Immunohistochemistry

Zebrafish larvae were fixed in 4% paraformaldehyde in PBS containing 4% sucrose for either 2 hours at room temperature or overnight at 4°C. Larvae were then washed 3 times (20 minutes each) in PBS containing 0.1% Tween20 (PBT), incubated for 30 minutes in distilled water, then incubated in antibody block (5% heat-inactivated goat serum in PBS containing 0.2% Triton, 1% DMSO, 0.02% sodium azide, and 0.2% BSA) for at least one hour at room temperature. Larvae were then incubated in rabbit anti-GFP diluted 1:500 in antibody block overnight at 4°C. The next day, larvae were once again washed 3 times (20 minutes each) in PBT, then incubated in a fluorescently-conjugated secondary antibody (Invitrogen, Alexa Fluor 488) diluted 1:1000 in antibody block for 4-5 hours at room temperature. From this point onward, larvae were protected

from light. Larvae were then rinsed 3 times (10 minutes each) in PBT and then stored in antibody block at 4°C until imaging. All wash and incubation steps occurred with rocking.

Click-iT

Cells that had incorporated F-ara-EdU were visualized via a Click-iT reaction. Following incubation in secondary antibody, larvae were washed 3 times (10 minutes each) in PBS, then incubated in 700 μL of a Click-iT reaction mix consisting of 2mM $CuSO_4$, 10 μM Alexa Fluor 555 azide, and 20 mM sodium ascorbate in PBS (made fresh) for 1 hour at room temperature. Larvae were then washed 6 times (20 minutes each) in PBT to ensure proper clearing of background labeling and stored in antibody block at 4°C until imaging.

Confocal Imaging

With the exception of the EdU experiment, all imaging was performed using an inverted Marianas spinning disk system (Intelligent Imaging Innovations, 3i) with an Evolve 10 MHz EMCCD camera (Photometrics) and a Zeiss C-Apochromat 63x/1.2W numerical aperture water objective. All imaging experiments were conducted with fixed larvae ages 3-8 dpf. Fish were placed in a chambered borosilicate coverglass (Lab-Tek) containing 2.5-2.5 mL E3 embryo medium and oriented on their sides with a slice anchor harp (Harvard Instruments). Imaging was performed at ambient temperature, generally 25°C. Fish were positioned on their sides against the cover glass in order to image the three cristae (anterior, lateral, and posterior). Cristae were imaged on each side of the fish. All imaging was performed with an intensification of 650, a gain of 3, and an exposure time between 25-1500 ms (depending on the brightness of the signal) with a 488 nm laser and a step size of 1 μm. All 3i Slidebook images were exported as .tif files to Fiji.

For the EdU experiment, imaging was performed on a Zeiss LSM 880 microscope with a Zeiss C-Apochromat 40x/1.2W numerical water objective (because the spinning disk was broken at the time). Fish were immersed in a solution of 50%glycerol/50% PBS, and then mounted on a plain microscope slide (Richard-Allen) beneath a triple wholemount coverslip. Imaging was performed at ambient temperature, generally 25°C. Fish were positioned on their sides against the cover glass in order to image the three cristae (anterior, lateral, and posterior). All imaging was performed at 4x digital zoom with master gain between 500-800 for 488 and 561 nm lasers, with a step size of 1 μm. All images were captured through the Zen Black software and opened in Fiji as .czi files.

Statistical Analysis

All statistical analyses were done with GraphPad Prism 6.0. The Kruskal-Wallis test, with a Dunn's post-test, was used for all comparisons. Statistical significance was set at $p = 0.05$.

3.5 Figures

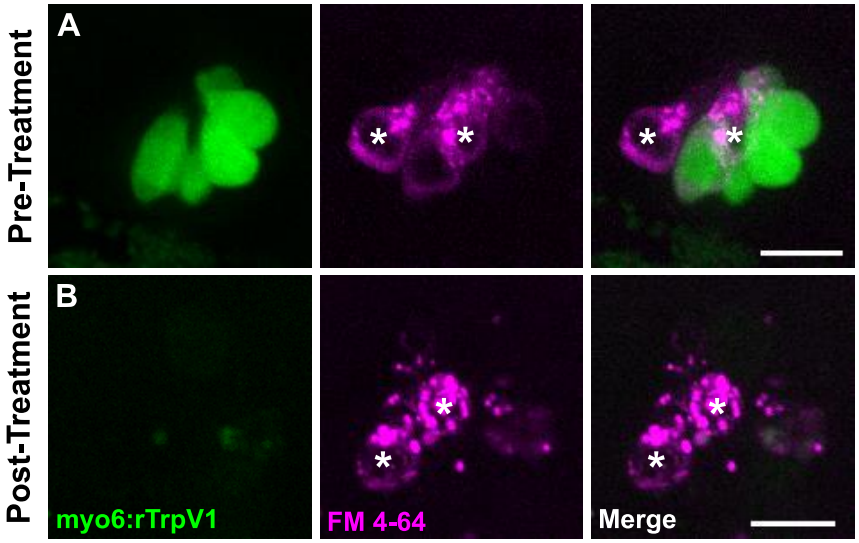

Figure 3.1. Capsaicin-mediated ablation of hair cells expressing mammalian TrpV1. **(A-B)** Maximum projections of an anterior neuromast transiently expressing myo6:rTrpV1 before (A) and after (B) treatment with 10 μM capsaicin. Myo6:rTrpV1-positive hair cells are shown in green, and hair cells labeled with the vital dye FM 4-64 are shown in magenta. Asterisks indicate hair cells not expressing rTrpV1. Capsaicin treatment ablates only those hair cells expressing myo6:rTrpV1 and does not impact neighboring hair cells (B). Scale bar = 10 μm.

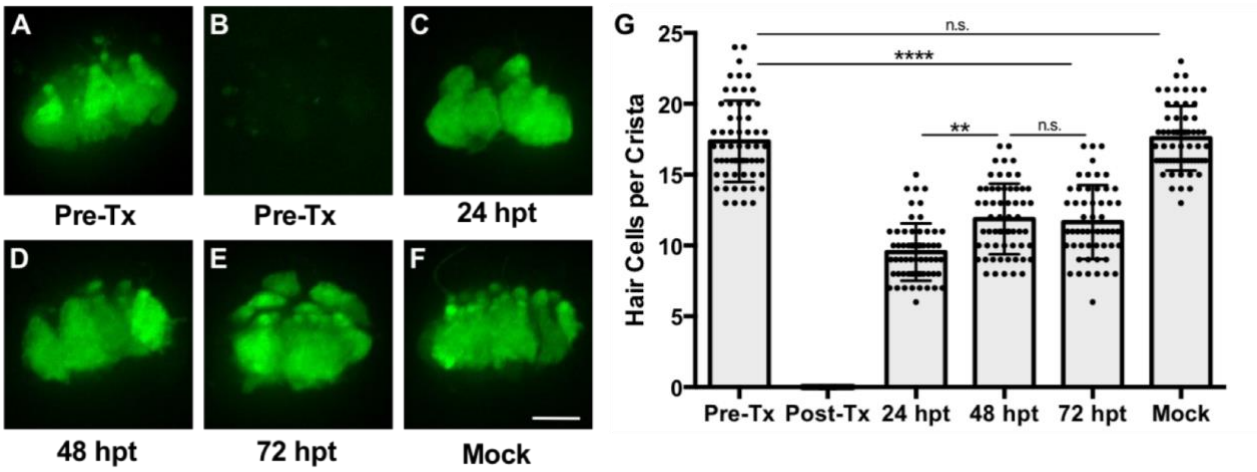

Figure 3.2. Inner ear hair cells regenerate after ablation. **(A-F)** Maximum projections of lateral cristae at different timepoints following capsaicin ablation. Hair cells expressing rTrpV1 are shown in green. Scale bar = 10 μm. **(G)** Total rTrpV1-positive hair cells per crista at different timepoints following ablation. Pre-Tx: 17.35 ± 2.86, n = 60 cristae; Post-Tx: 0 ± 0, n = 60 cristae; 24 hpt: 9.53 ± 2.02, n = 60 cristae; 48 hpt: 11.87 ± 2.49, n = 60 cristae; 72 hpt: 11.65 ± 2.61, n = 54 cristae; Mock: 17.57 ± 2.27, n = 60 cristae; mean ± SD; Kruskal-Wallis test, Dunn's post-test, $p < 0.0001$ (Pre-Tx vs. 24/48/72 hpt, Post-Tx vs. everything, Mock vs. 24/48/72 hpt), $p > 0.9999$ (Pre-Tx vs. Mock, 48 hpt vs. 72 hpt), $p = 0.0085$ (24 hpt vs. 48 hpt), $p = 0.0281$ (24 hpt vs. 72 hpt).

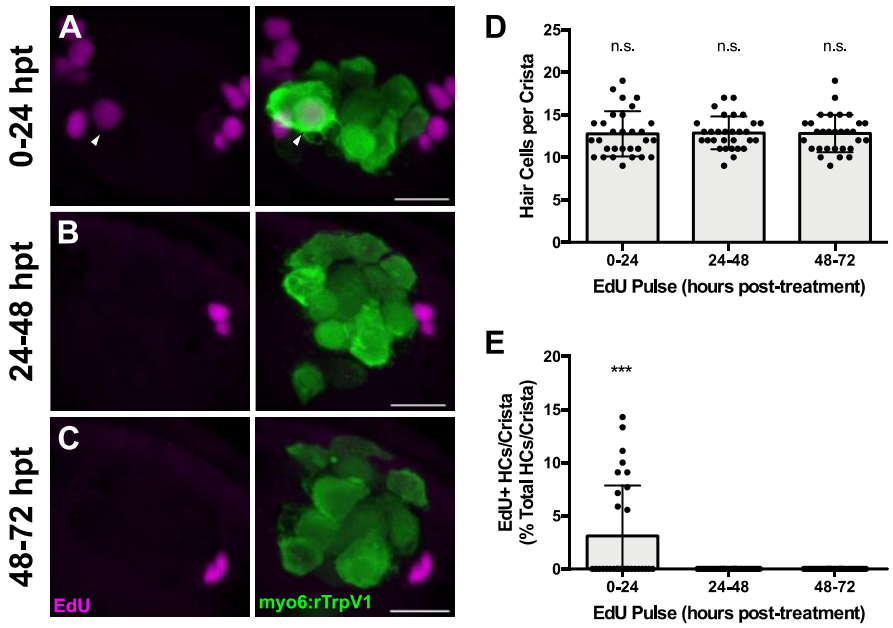

Figure 3.3. Inner ear hair cell regeneration occurs primarily via transdifferentiation. **(A-C)** Maximum projections of lateral cristae 72 hours post-ablation following EdU incubation from 0-24 hpt (A), 24-48 hpt (B), and 48-72 hpt (C). Myo6:rTrpV1-positive hair cells are shown in green, and EdU-positive cells are shown in magenta. Arrowheads indicate EdU-positive hair cells. Scale bar = 10 μm. **(D)** Total number of hair cells per crista from each group. 0-24 hpt: 12.77 ± 2.66, n = 30 cristae; 24-48 hpt: 12.87 ± 1.93, n = 30 cristae; 48-72 hpt: 12.80 ± 2.20, n = 30 cristae; mean ± SD; Kruskal-Wallis test, Dunn's post-test, $p > 0.9999$ (all comparisons). **(E)** Percentage of hair cells per cristae labeled with EdU from each group. 0-24 hpt: 3.11 ± 4.76, n = 30 cristae; 24-48 hpt: 0 ± 0, n = 30 cristae; 48-72 hpt: 0 ± 0, n = 30 cristae; mean ± SD; Kruskal-Wallis test, Dunn's post-test, $p = 0.0001$ (0-24 hpt vs. 24-48/48-72 hpt), $p > 0.9999$ (24-48 hpt vs. 48-72 hpt).

CHAPTER 4

CONCLUSIONS AND FUTURE DIRECTIONS

In the work showcased in this thesis, I have demonstrated that there are functionally distinct progenitor populations in the neuromasts of the zebrafish lateral line (Chapter 2). Utilizing novel CRISPR transgenesis technology and fate mapping studies, I selectively labeled distinct subsets of support cells (peripheral, anteroposterior (AP), and dorsoventral (DV)) and identified differences in regenerative capacities. The peripheral population does not contribute to hair cell regeneration, even after Notch signaling is inhibited. The AP population generates a small proportion of regenerated hair cells but is heavily regulated by Notch signaling, as inhibition of Notch greatly increases its contribution to hair cell regeneration. The DV population comprises the majority of hair cell progenitors and is also regulated by Notch signaling. Furthermore, this population is itself capable of regenerating, and can be replenished by the peripheral and AP populations. The AP and DV population also seem to be independently regulated, perhaps via Notch signaling, indicating that lateral line neuromasts may utilize different progenitors to respond to different types of damage. Through this work, I have not only identified molecular markers of progenitor cells within the neuromast, but have also definitively shown that hair cell progenitors are replaced by other support cells. I have also begun to characterize hair cell regeneration in the larval inner ear, demonstrating that regeneration occurs primarily via transdifferentiation (Chapter 3). In spite of these achievements, there are a number of questions that remain unanswered. I addressed the inner ear regeneration experiments that need to be done at the end of Chapter 3, but here I will address some future studies involving further characterization of lateral line progenitor populations.

4.1 Profiling of Distinct Progenitor Populations

As mentioned in Chapter 2, the transgenic lines I developed to label distinct subsets of support cells were very useful for examining the role of those populations of cells, but not the role of the genes that were driving transgene expression. The actual functions of *sfrp1a*, *tnfsf10l3*, or *sost* within those cells were irrelevant, as I was interested in how the population of cells themselves responded to hair cell death. However, since there are clear differences in progenitor function between these populations, it is important to determine which genes and signaling pathways are utilized by these different populations. To do so, we could utilize the wide array of genetic profiling techniques, such as RNAseq or ATACseq, on support cells isolated from these different transgenic lines at different stages during regeneration. Since our transgenes label specific subsets of support cells, we would likely be dealing with a fairly homogeneous population of cells after sorting, and so a bulk RNAseq approach would likely be sufficient. However, the *sost*:nlsEos line is more heterogeneous than the other lines, since it labels both immature and mature hair cell progenitors. In this case, a single cell RNAseq approach would be ideal. In order to further assess the differences between these immature and mature hair cell progenitors, we could also cross the *sost*:nlsEos and *sost*:NTR-GFP lines and photoconvert them before cell sorting. The expression profiles of the cells that are both green and red (expressing both NTR-GFP and nlsEos) could then be compared to cells that are only red (expressing only nlsEos). These differences could also be compared to any differences in expression profiles seen in the single cell data from the *sost*:nlsEos line. Upon identifying any differentially expressed genes between these progenitors, we could then target those genes via CRISPR-mediated transgenesis in order to specifically label immature or mature hair cell progenitors *in vivo*. Furthermore, analyzing the expression profiles from the *sfrp1a*, *tnfsf10l3*,

and *sost* lines would not only provide a greater understanding of the genes and pathways regulating these different progenitor populations (for instance, would *sfrp1a*:nlsEos cells be enriched for genes involved in quiescence or for genes typically associated with stemness?), but could also provide targets for loss-of-function studies. In addition, employing ATACseq or ChiPseq would begin to provide an understanding of the epigenetic regulation of progenitor state within the neuromast.

4.2 The Impact of Ablating the *sfrp1a* Population

In Chapter 2, I demonstrated that ablating the *sost*:NTR-GFP population significantly reduced hair cell regeneration. Moving forward, it will be important to assess the impact of ablating the other support cell populations as well. Despite my best efforts, I was unable to knock in my NTR-GFP construct into the *tnfsf10l3* locus. However, I was able to generate a *sfrp1a*:NTR-GFP line. The NTR-GFP transgene recapitulated the expression seen in the GFP and nlsEos lines, being expressed in the peripheral mantle cells of neuromasts. It is important to note that, in all three *sfrp1a* lines, the transgene was also expressed in interneuromast cells and inner ear support cells. Unfortunately, the expression of NTR-GFP was significantly lower in the mantle cells of neuromasts compared to other cell populations, even in homozygous fish. As a result of this low NTR expression, the mantle cells could not be ablated by metronidazole treatments, and I was thus unable to assess the impact of *sfrp1a*:NTR-GFP ablation on lateral line hair cell regeneration (which is why it was not discussed in Chapter 2).

However, metronidazole treatment was sufficient to ablate the interneuromast cells and inner ear support cells, and I observed some very interesting consequences as a result. First, ablation of these cell populations at 3 dpf resulted in permanent loss of NTR-GFP-labeled

interneuromast cells and inner ear support cells. Following Mtz treatment, larvae also showed significant vestibular defects, similar to those observed in myo6:rTrpV1 larvae after capsaicin treatment (Chapter 3). I grew these fish up in our fish facility and examined their posterior lateral lines at 14 dpf. As zebrafish age, their lateral line systems grow and become more complex. During this process, interneuromast cells serve as progenitors for entirely new neuromasts, known as intercalary neuromasts, which are generated in between existing neuromasts that were deposited by the migrating primordia (Nuñez et al., 2009). These juvenile fish were incubated in the vital dye FM 1-43 to visualize hair cells, then anesthetized and placed under a dissection microscope. Fish that were not treated with Mtz had about 20 neuromasts per trunk, whereas Mtz-treated fish had only 5 (Fig. 4.1; 19.5 ± 2.42 [Mock] vs. 5.5 ± 0.45 [Mtz], $p = 0.0022$). These results indicate that Mtz treatment truly did permanently ablate the interneuromast population, and the loss prevented the formation of future neuromasts during later development. The only neuromasts that were present on the trunks of Mtz-treated fish were the neuromasts that had already developed at the time of ablation (neuromasts derived from the initial primordium). Interestingly, there was no noticeable difference in neuromast number between mock and Mtz-treated fish on the head. These neuromasts, which comprise the anterior lateral line, develop in a different manner compared to the neuromasts on the trunk (the posterior lateral line), and this suggests that interneuromast cells on the head are not necessary for later neuromast development. Differences between anterior and posterior interneuromast cells could be characterized by isolated *sfrp1a* cells from the head vs. the trunk and profiled via single cell RNAseq.

As the lateral line grows with age, neuromasts of the posterior lateral line are organized in small clusters known as stitches. These stitches are formed via budding of new neuromasts from existing neuromasts (Nuñez et al., 2009). This budding process is also responsible for the

generation of neuromasts along the rays of the caudal fin, known as the caudal lateral line. These caudal fin neuromasts are derived from the neuromasts located at the tip of the tail (also known as the terminal cluster) (Dufourcq et al., 2006). Even as adults, the Mtz-treated fish still had far fewer neuromasts per trunk (still about 5). However, the neuromasts that were present were able to form stitches. These fish were also able to develop a caudal lateral line (anecdotal). I believe this is because the NTR-GFP-positive cells within the neuromasts themselves were not ablated and were thus able to serve as the source of these new neuromasts. This would be consistent with previous reports of mantle cells being responsible for budding (Dufourcq et al., 2006). Previous studies in both zebrafish and axolotls have also demonstrated that, following tail amputation, mantle cells of the most posterior neuromast generates a regenerative placode which migrates along the regenerating tail and replenishes the neuromasts that had been lost (Dufourcq et al., 2006; Jones & Corwin, 1993). A similar experiment could be performed with *sfrp1a*:NTR-GFP fish, both with and without Mtz ablation. However, since the GFP-positive mantle cells cannot be ablated by our Mtz paradigm, I would expect caudal neuromast regeneration to be unaffected following NTR-GFP ablation. But perhaps NTR-GFP levels are higher in the mantle cells of adult fish.

Interestingly, the vestibular defects first observed in larvae following Mtz-treatment persisted into adulthood. Mtz-treated fish had difficulty swimming upright, and would often sink to the bottom of their tank before jerking upward haphazardly. In one extreme case, a fish would sporadically begin swimming rapidly in a tight circle, resembling a helicopter. That these vestibular defects persist into adulthood indicates that, like the interneuromast cells, the *sfrp1a*:NTR-GFP support cells in the inner ear are not replaced following ablation. The widespread loss of inner ear support cells presumably leads to the loss of inner ear hair cells and

thus the vestibular defects (although I haven't yet tested this). As posited in Chapter 3, if inner ear support cells transdifferentiate into new hair cells without replacement, then the regenerative capacity of the inner ear could be diminished after repeated hair cell ablation. The fact that these inner ear support cells are not replaced after damage is consistent with this hypothesis. Moving forward, the extent of *sfrp1a* transgene expression throughout the inner ear epithelia will need to be examined, as will whether or not *sfrp1a*:nlsEos cells serve as inner ear hair cell progenitors.

4.3 Figures

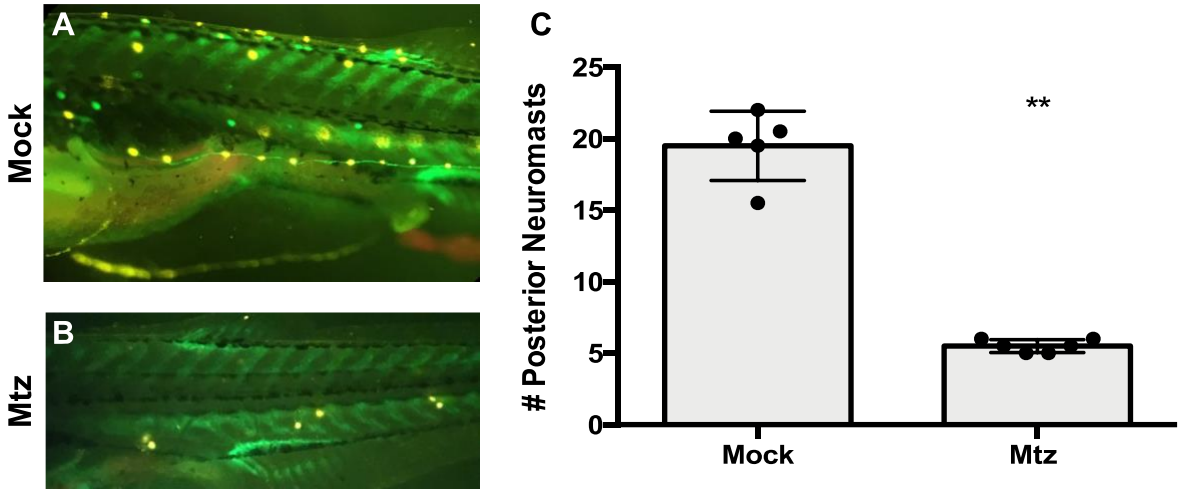

Figure 4.1 Ablation of *sfrp1a*:NTR-GFP cells permanently reduces number of posterior neuromasts during development. **(A-B)** Images of the trunk of a 14 dpf *sfrp1a*:NTR-GFP fish in the absence of (A) or following Mtz treatment at 3 dpf (B). Yellow dots indicate hair cells labeled with the vital dye FM 1-43. **(C)** Total number of neuromasts in the posterior lateral line per fish. Each dot represents an average of both sides of a fish. Mock: 19.5 ± 2.42, n = 5 fish; Mtz: 5.5 ± 0.45, n = 6 fish; mean ± SD; Mann Whitney U test; p = 0.0022.

BIBLIOGRAPHY

Adler, H. J., & Raphael, Y. (1996). New hair cells arise from supporting cell conversion in the acoustically damaged chick inner ear. *Neuroscience Letters*, *205*(1), 17–20. Retrieved from http://www.ncbi.nlm.nih.gov/pubmed/8867010

Agrawal, Y., Carey, J. P., Della Santina, C. C., Schubert, M. C., & Minor, L. B. (2009). Disorders of Balance and Vestibular Function in US Adults. *Archives of Internal Medicine*, *169*(10), 938. http://doi.org/10.1001/archinternmed.2009.66

Baird, R. A., Burton, M. D., Fashena, D. S., Naeger, R. A., & Naeger, R. A. (2000). Hair cell recovery in mitotically blocked cultures of the bullfrog saccule. *Proceedings of the National Academy of Sciences*, *97*(22), 11722–11729. http://doi.org/10.1073/pnas.97.22.11722

Baird, R. A., Steyger, P. S., & Schuff, N. R. (1996). Mitotic and nonmitotic hair cell regeneration in the bullfrog vestibular otolith organs. *Annals of the New York Academy of Sciences*, *781*, 59–70. Retrieved from http://www.ncbi.nlm.nih.gov/pubmed/8694449

Barker, N., van Es, J. H., Kuipers, J., Kujala, P., van den Born, M., Cozijnsen, M., … Clevers, H. (2007). Identification of stem cells in small intestine and colon by marker gene Lgr5. *Nature*, *449*(7165), 1003–1007. http://doi.org/10.1038/nature06196

Bermingham, N. A., Hassan, B. A., Price, S. D., Vollrath, M. A., Ben-Arie, N., Eatock, R. A., … Zoghbi, H. Y. (1999). Math1: an essential gene for the generation of inner ear hair cells. *Science (New York, N.Y.)*, *284*(5421), 1837–41. Retrieved from http://www.ncbi.nlm.nih.gov/pubmed/10364557

Bever, M. M., & Fekete, D. M. (2002). Atlas of the developing inner ear in zebrafish. *Developmental Dynamics*, *223*(4), 536–543. http://doi.org/10.1002/dvdy.10062

Bhandiwad, A. A., Raible, D. W., Rubel, E. W., & Sisneros, J. A. (2018). Noise-Induced Hypersensitization of the Acoustic Startle Response in Larval Zebrafish. *Journal of the Association for Research in Otolaryngology*, 1–12. http://doi.org/10.1007/s10162-018-00685-0

Bhandiwad, A. A., Zeddies, D. G., Raible, D. W., Rubel, E. W., & Sisneros, J. A. (2013). Auditory sensitivity of larval zebrafish (Danio rerio) measured using a behavioral prepulse inhibition assay. *The Journal of Experimental Biology*, *216*(Pt 18), 3504–13. http://doi.org/10.1242/jeb.087635

Bucks, S. A., Cox, B. C., Vlosich, B. A., Manning, J. P., Nguyen, T. B., & Stone, J. S. (2017). Supporting cells remove and replace sensory receptor hair cells in a balance organ of adult mice. *ELife*, *6*. http://doi.org/10.7554/eLife.18128

Burns, J. C., Collado, M. S., Oliver, E. R., & Corwin, J. T. (2013). Specializations of intercellular junctions are associated with the presence and absence of hair cell regeneration in ears from six vertebrate classes. *Journal of Comparative Neurology*, *521*(6), 1430–1448. http://doi.org/10.1002/cne.23250

Burns, J. C., & Corwin, J. T. (2014). Responses to cell loss become restricted as the supporting cells in mammalian vestibular organs grow thick junctional actin bands that develop high stability. *The Journal of Neuroscience : The Official Journal of the Society for*

Neuroscience, *34*(5), 1998–2011. http://doi.org/10.1523/JNEUROSCI.4355-13.2014

Burns, J. C., On, D., Baker, W., Collado, M. S., & Corwin, J. T. (2012). Over Half the Hair Cells in the Mouse Utricle First Appear After Birth, with Significant Numbers Originating from Early Postnatal Mitotic Production in Peripheral and Striolar Growth Zones. *Journal of the Association for Research in Otolaryngology*, *13*(5), 609–627. http://doi.org/10.1007/s10162-012-0337-0

Burns, J., Christophel, J. J., Collado, M. S., Magnus, C., Carfrae, M., Corwin, J. T., & Corwin, J. T. (2008). Reinforcement of cell junctions correlates with the absence of hair cell regeneration in mammals and its occurrence in birds. *The Journal of Comparative Neurology*, *511*(3), 396–414. http://doi.org/10.1002/cne.21849

Carey, J. P., Fuchs, A. F., & Rubel, E. W. (1996). Hair cell regeneration and recovery of the vestibuloocular reflex in the avian vestibular system. *Journal of Neurophysiology*, *76*(5), 3301–3312. http://doi.org/10.1152/jn.1996.76.5.3301

Chen, S., Chiu, C. N., McArthur, K. L., Fetcho, J. R., & Prober, D. A. (2016). TRP channel mediated neuronal activation and ablation in freely behaving zebrafish. *Nature Methods*, *13*(2), 147–50. http://doi.org/10.1038/nmeth.3691

Choi, R., & Goldstein, B. J. (2018). Olfactory epithelium: Cells, clinical disorders, and insights from an adult stem cell niche. *Laryngoscope Investigative Otolaryngology*, *3*(1), 35–42. http://doi.org/10.1002/lio2.135

Collado, M. S., Thiede, B. R., Baker, W., Askew, C., Igbani, L. M., & Corwin, J. T. (2011). The Postnatal Accumulation of Junctional E-Cadherin Is Inversely Correlated with the Capacity for Supporting Cells to Convert Directly into Sensory Hair Cells in Mammalian Balance Organs. *Journal of Neuroscience*, *31*(33), 11855–11866. http://doi.org/10.1523/JNEUROSCI.2525-11.2011

Corwin, J. T., & Cotanche, D. A. (1988). Regeneration of sensory hair cells after acoustic trauma. *Science (New York, N.Y.)*, *240*(4860), 1772–4. Retrieved from http://www.ncbi.nlm.nih.gov/pubmed/3381100

Cotanche, D. A. (1987). Regeneration of hair cell stereociliary bundles in the chick cochlea following severe acoustic trauma. *Hearing Research*, *30*(2–3), 181–95. Retrieved from http://www.ncbi.nlm.nih.gov/pubmed/3680064

Cruz, I. A., Kappedal, R., Mackenzie, S. M., Hailey, D. W., Hoffman, T. L., Schilling, T. F., & Raible, D. W. (2015). Robust regeneration of adult zebrafish lateral line hair cells reflects continued precursor pool maintenance. *Developmental Biology*, *402*(2), 229–238. http://doi.org/10.1016/j.ydbio.2015.03.019

Cruz, R. M., Lambert, P. R., & Rubel, E. W. (1987). Light microscopic evidence of hair cell regeneration after gentamicin toxicity in chick cochlea. *Archives of Otolaryngology--Head & Neck Surgery*, *113*(10), 1058–62. Retrieved from http://www.ncbi.nlm.nih.gov/pubmed/3620125

Curado, S., Anderson, R. M., Jungblut, B., Mumm, J., Schroeter, E., & Stainier, D. Y. R. (2007). Conditional targeted cell ablation in zebrafish: A new tool for regeneration studies.

Developmental Dynamics, *236*(4), 1025–1035. http://doi.org/10.1002/dvdy.21100

Daudet, N., Gibson, R., Shang, J., Bernard, A., Lewis, J., & Stone, J. (2009). Notch regulation of progenitor cell behavior in quiescent and regenerating auditory epithelium of mature birds. *Developmental Biology*, *326*(1), 86–100. http://doi.org/10.1016/j.ydbio.2008.10.033

Daudet, N., & Lewis, J. (2005). Two contrasting roles for Notch activity in chick inner ear development: specification of prosensory patches and lateral inhibition of hair-cell differentiation. *Development (Cambridge, England)*, *132*(3), 541–551. http://doi.org/10.1242/dev.01589

Dufourcq, P., Roussigné, M., Blader, P., Rosa, F., Peyrieras, N., & Vriz, S. (2006). Mechano-sensory organ regeneration in adults: The zebrafish lateral line as a model. *Molecular and Cellular Neuroscience*, *33*(2), 180–187. http://doi.org/10.1016/J.MCN.2006.07.005

Forge, A., Li, L., & Nevill, G. (1998). Hair cell recovery in the vestibular sensory epithelia of mature guinea pigs. *The Journal of Comparative Neurology*, *397*(1), 69–88. Retrieved from http://www.ncbi.nlm.nih.gov/pubmed/9671280

Gau, P., Poon, J., Ufret-Vincenty, C., Snelson, C. D., Gordon, S. E., Raible, D. W., & Dhaka, A. (2013). The Zebrafish Ortholog of TRPV1 Is Required for Heat-Induced Locomotion. *Journal of Neuroscience*, *33*(12), 5249–5260. http://doi.org/10.1523/JNEUROSCI.5403-12.2013

Girod, D. A., Tucci, D. L., & Rubel, E. W. (1991). Anatomical Correlates of Functional Recovery in the Avian Inner Ear Following Aminoglycoside Ototoxicity. *The Laryngoscope*, *101*(11), 1139???1149. http://doi.org/10.1288/00005537-199111000-00001

Goman, A. M., & Lin, F. R. (2016). Prevalence of Hearing Loss by Severity in the United States. *American Journal of Public Health*, *106*(10), 1820–2. http://doi.org/10.2105/AJPH.2016.303299

Goode, C. T., Carey, J. P., Fuchs, A. F., & Rubel, E. W. (1999). Recovery of the Vestibulocolic Reflex After Aminoglycoside Ototoxicity in Domestic Chickens. *Journal of Neurophysiology*, *81*(3), 1025–1035. http://doi.org/10.1152/jn.1999.81.3.1025

Grant, K. a., Raible, D. W., & Piotrowski, T. (2005). Regulation of latent sensory hair cell precursors by glia in the zebrafish lateral line. *Neuron*, *45*(1), 69–80. http://doi.org/10.1016/j.neuron.2004.12.020

Guerra, E., de Lara, J., Malizia, A., & Díaz, P. (2009). Supporting user-oriented analysis for multi-view domain-specific visual languages. *Information and Software Technology*. http://doi.org/10.1016/j.infsof.2008.09.005

Haddon, C., Jiang, Y. J., Smithers, L., & Lewis, J. (1998). Delta-Notch signalling and the patterning of sensory cell differentiation in the zebrafish ear: evidence from the mind bomb mutant. *Development (Cambridge, England)*, *125*(23), 4637–4644.

Harris, J. A., Cheng, A. G., Cunningham, L. L., MacDonald, G., Raible, D. W., & Rubel, E. W. (2003). Neomycin-induced hair cell death and rapid regeneration in the lateral line of zebrafish (Danio rerio). *Journal of the Association for Research in Otolaryngology : JARO*, *4*(2), 219–34. http://doi.org/10.1007/s10162-002-3022-x

Hartman, B. H., Basak, O., Nelson, B. R., Taylor, V., Bermingham-Mcdonogh, O., & Reh, T. a. (2009). Hes5 expression in the postnatal and adult mouse inner ear and the drug-damaged cochlea. *JARO - Journal of the Association for Research in Otolaryngology*, *10*(3), 321–340. http://doi.org/10.1007/s10162-009-0162-2

Hernández, P. P., Moreno, V., Olivari, F. a., & Allende, M. L. (2006). Sub-lethal concentrations of waterborne copper are toxic to lateral line neuromasts in zebrafish (Danio rerio). *Hearing Research*, *213*(1–2), 1–10. http://doi.org/10.1016/j.heares.2005.10.015

Hernández, P. P., Olivari, F. a, Sarrazin, A. F., Sandoval, P. C., & Allende, M. L. (2007). Regeneration in zebrafish lateral line neuromasts: expression of the neural progenitor cell marker sox2 and proliferation-dependent and-independent mechanisms of hair cell renewal. *Developmental Neurobiology*, *67*(5), 637–654. http://doi.org/10.1002/dneu

Hsu, Y.-C., Li, L., & Fuchs, E. (2014). Emerging interactions between skin stem cells and their niches. *Nature Medicine*, *20*(8), 847–856. http://doi.org/10.1038/nm.3643

Ito, M., Liu, Y., Yang, Z., Nguyen, J., Liang, F., Morris, R. J., & Cotsarelis, G. (2005). Stem cells in the hair follicle bulge contribute to wound repair but not to homeostasis of the epidermis. *Nature Medicine*, *11*(12), 1351–1354. http://doi.org/10.1038/nm1328

Iwai, N., Zhou, Z., Roop, D. R., & Behringer, R. R. (2008). Horizontal basal cells are multipotent progenitors in normal and injured adult olfactory epithelium. *Stem Cells (Dayton, Ohio)*, *26*(5), 1298–306. http://doi.org/10.1634/stemcells.2007-0891

Jiang, T., Kindt, K., & Wu, D. K. (2017). Transcription factor Emx2 controls stereociliary bundle orientation of sensory hair cells. *ELife*, *6*. http://doi.org/10.7554/eLife.23661

Jones, J., & Corwin, J. (1993). Replacement of lateral line sensory organs during tail regeneration in salamanders: identification of progenitor cells and analysis of leukocyte activity. *Journal of Neuroscience*, *13*(3), 1022–1034. http://doi.org/10.1523/JNEUROSCI.13-03-01022.1993

Jørgensen, J. M., & Mathiesen, C. (1988). The avian inner ear. Continuous production of hair cells in vestibular sensory organs, but not in the auditory papilla. *Die Naturwissenschaften*, *75*(6), 319–20. Retrieved from http://www.ncbi.nlm.nih.gov/pubmed/3205314

Kiernan, A. E., Xu, J., & Gridley, T. (2006). The notch ligand JAG1 is required for sensory progenitor development in the mammalian inner ear. *PLoS Genetics*, *2*(1), 27–38. http://doi.org/10.1371/journal.pgen.0020004

Kimura, Y., Hisano, Y., Kawahara, A., & Higashijima, S.-I. (2014). Efficient generation of knock-in transgenic zebrafish carrying reporter/driver genes by CRISPR/Cas9-mediated genome engineering. http://doi.org/10.1038/srep06545

Ledent, V. (2002). Postembryonic development of the posterior lateral line in zebrafish. *Development*, *129*(3).

Leung, C. T., Coulombe, P. A., & Reed, R. R. (2007). Contribution of olfactory neural stem cells to tissue maintenance and regeneration. *Nature Neuroscience*, *10*(6), 720–726. http://doi.org/10.1038/nn1882

Li, L., & Forge, A. (1997). Morphological evidence for supporting cell to hair cell conversion in

the mammalian utricular macula. *International Journal of Developmental Neuroscience : The Official Journal of the International Society for Developmental Neuroscience*, *15*(4–5), 433–46. Retrieved from http://www.ncbi.nlm.nih.gov/pubmed/9263024

Lin, V., Golub, J. S., Nguyen, T. B., Hume, C. R., Oesterle, E. C., & Stone, J. S. (2011). Inhibition Of Notch Activity Promotes Nonmitotic Regeneration of Hair Cells in the Adult Mouse Utricles. *Journal of Neuroscience*, *31*(43), 15329–15339. http://doi.org/10.1523/JNEUROSCI.2057-11.2011

Linbo, T. L., Stehr, C. M., Incardona, J. P., & Scholz, N. L. (2006). Dissolved copper triggers cell death in the peripheral mechanosensory system of larval fish. *Environmental Toxicology and Chemistry*, *25*(2), 597–603. Retrieved from http://www.ncbi.nlm.nih.gov/pubmed/16519324

López-Schier, H., & Hudspeth, A. J. (2006). A two-step mechanism underlies the planar polarization of regenerating sensory hair cells. *Proceedings of the National Academy of Sciences of the United States of America*, *103*(49), 18615–18620. http://doi.org/10.1073/pnas.0608536103

López-Schier, H., Starr, C. J., Kappler, J. a., Kollmar, R., & Hudspeth, a. J. (2004). Directional cell migration establishes the axes of planar polarity in the posterior lateral-Line organ of the zebrafish. *Developmental Cell*, *7*(3), 401–412. http://doi.org/10.1016/j.devcel.2004.07.018

Ma, E. Y., Rubel, E. W., & Raible, D. W. (2008). Notch Signaling Regulates the Extent of Hair Cell Regeneration in the Zebrafish Lateral Line. *The Journal of Neuroscience*, *28*(9), 2261–2273. http://doi.org/10.1523/JNEUROSCI.4372-07.2008

Mackenzie, S. M., & Raible, D. W. (2012). Proliferative Regeneration of Zebrafish Lateral Line Hair Cells after Different Ototoxic Insults. *PLoS ONE*, *7*(10), 1–8. http://doi.org/10.1371/journal.pone.0047257

Matsuda, M., & Chitnis, A. B. (2010). Atoh1a expression must be restricted by Notch signaling for effective morphogenesis of the posterior lateral line primordium in zebrafish. *Development (Cambridge, England)*, *137*(20), 3477–3487. http://doi.org/10.1242/dev.052761

McHenry, M. J., Feitl, K. E., Strother, J. A., & Van Trump, W. J. (2009). Larval zebrafish rapidly sense the water flow of a predator's strike. *Biology Letters*, *5*(4), 477–479. http://doi.org/10.1098/rsbl.2009.0048

McMenamin, S. K., Bain, E. J., McCann, A. E., Patterson, L. B., Eom, D. S., Waller, Z. P., … Parichy, D. M. (2014). Thyroid hormone-dependent adult pigment cell lineage and pattern in zebrafish. *Science (New York, N.Y.)*, *345*(6202), 1358. http://doi.org/10.1126/SCIENCE.1256251

Mellado Lagarde, M. M., Wan, G., Zhang, L., Gigliello, A. R., McInnis, J. J., Zhang, Y., … Corfas, G. (2014). Spontaneous regeneration of cochlear supporting cells after neonatal ablation ensures hearing in the adult mouse. *Proceedings of the National Academy of Sciences of the United States of America*, *111*(47), 16919–24.

http://doi.org/10.1073/pnas.1408064111

Millimaki, B. B., Sweet, E. M., & Riley, B. B. (2010). Sox2 is required for maintenance and regeneration, but not initial development, of hair cells in the zebrafish inner ear. *Developmental Biology*, *338*(2), 262–9. http://doi.org/10.1016/j.ydbio.2009.12.011

Mirkovic, I., Pylawka, S., & Hudspeth, a. J. (2012). Rearrangements between differentiating hair cells coordinate planar polarity and the establishment of mirror symmetry in lateral-line neuromasts. *Biology Open*, *1*(5), 498–505. http://doi.org/10.1242/bio.2012570

Mizutari, K., Fujioka, M., Hosoya, M., Bramhall, N., Okano, H. H. J., Okano, H. H. J., & Edge, A. S. B. (2013). Notch Inhibition Induces Cochlear Hair Cell Regeneration and Recovery of Hearing after Acoustic Trauma. *Neuron*, *77*(1), 58–69. http://doi.org/10.1016/j.neuron.2012.10.032

Neef, A. B., & Luedtke, N. W. (2011). Dynamic metabolic labeling of DNA in vivo with arabinosyl nucleosides. *Proceedings of the National Academy of Sciences*, *108*(51), 20404–20409. http://doi.org/10.1073/pnas.1101126108

Nicolson, T. (2005). The Genetics of Hearing and Balance in Zebrafish. *Annual Review of Genetics*, *39*(1), 9–22. http://doi.org/10.1146/annurev.genet.39.073003.105049

Nuñez, V. a., Sarrazin, A. F., Cubedo, N., Allende, M. L., Dambly-Chaudière, C., & Ghysen, A. (2009). Postembryonic development of the posterior lateral line in the zebrafish. *Evolution and Development*, *11*(4), 391–404. http://doi.org/10.1111/j.1525-142X.2009.00346.x

Oesterle, E. C., Cunningham, D. E., Westrum, L. E., & Rubel, E. W. (2003). Ultrastructural analysis of [3H]thymidine-labeled cells in the rat utricular macula. *The Journal of Comparative Neurology*, *463*(2), 177–195. http://doi.org/10.1002/cne.10756

Ogata, Y., Slepecky, N. B., & Takahashi, M. (1999). Study of the gerbil utricular macula following treatment with gentamicin, by use of bromodeoxyuridine and calmodulin immunohistochemical labelling. *Hearing Research*, *133*(1–2), 53–60. Retrieved from http://www.ncbi.nlm.nih.gov/pubmed/10416864

Ota, S., Taimatsu, K., Yanagi, K., Namiki, T., Ohga, R., Higashijima, S., & Kawahara, A. (2016). Functional visualization and disruption of targeted genes using CRISPR/Cas9-mediated eGFP reporter integration in zebrafish. *Scientific Reports*, *6*(1), 34991. http://doi.org/10.1038/srep34991

Ou, H. C., Raible, D. W., & Rubel, E. W. (2007). Cisplatin-induced hair cell loss in zebrafish (Danio rerio) lateral line. *Hearing Research*, *233*(1–2), 46–53. http://doi.org/10.1016/j.heares.2007.07.003

Pinto-Teixeira, F., Viader-Llargues, O., Torres-Mejia, E., Turan, M., Gonzalez-Gualda, E., Pola-Morell, L., & Lopez-Schier, H. (2015). Inexhaustible hair-cell regeneration in young and aged zebrafish. *Biology Open*, *4*(7), 903–909. http://doi.org/10.1242/bio.012112

Roberson, D. F., Weisleder, P., Bohrer, P. S., & Rubel, E. W. (1992). Ongoing production of sensory cells in the vestibular epithelium of the chick. *Hearing Research*, *57*(2), 166–74. Retrieved from http://www.ncbi.nlm.nih.gov/pubmed/1733910

Roberson, D. W., Alosi, J. A., & Cotanche, D. A. (2004). Direct transdifferentiation gives rise to

the earliest new hair cells in regenerating avian auditory epithelium. *Journal of Neuroscience Research*, *78*(4), 461–471. http://doi.org/10.1002/jnr.20271

Roberson, D. W., & Rubel, E. W. (1994). Cell division in the gerbil cochlea after acoustic trauma. *The American Journal of Otology*, *15*(1), 28–34. Retrieved from http://www.ncbi.nlm.nih.gov/pubmed/8109626

Romero-Carvajal, A., Navajas Acedo, J., Jiang, L., Kozlovskaja-Gumbriene, A., Alexander, R., Li, H., … Piotrowski, T. (2015). Regeneration of Sensory Hair Cells Requires Localized Interactions between the Notch and Wnt Pathways. *Developmental Cell*, *34*(3), 267–282. http://doi.org/10.1016/j.devcel.2015.05.025

Rompolas, P., & Greco, V. (2014). Stem cell dynamics in the hair follicle niche. *Seminars in Cell & Developmental Biology*, *25–26*, 34–42. http://doi.org/10.1016/j.semcdb.2013.12.005

Sans, A., & Chat, M. (1982). Analysis of temporal and spatial patterns of rat vestibular hair cell differentiation by tritiated thymidine radioautography. *The Journal of Comparative Neurology*, *206*(1), 1–8. http://doi.org/10.1002/cne.902060102

Santos, A. J. M., Lo, Y.-H., Mah, A. T., & Kuo, C. J. (2018). The Intestinal Stem Cell Niche: Homeostasis and Adaptations. *Trends in Cell Biology*, *0*(0). http://doi.org/10.1016/j.tcb.2018.08.001

Sapède, D., Gompel, N., Dambly-Chaudière, C., & Ghysen, A. (2002). Cell migration in the postembryonic development of the fish lateral line. *Development (Cambridge, England)*, *129*(3), 605–15. Retrieved from http://www.ncbi.nlm.nih.gov/pubmed/11830562

Schuck, J. B., & Smith, M. E. (2009). Cell proliferation follows acoustically-induced hair cell bundle loss in the zebrafish saccule. *Hearing Research*, *253*(1–2), 67–76. http://doi.org/10.1016/j.heares.2009.03.008

Schwob, J. E., Jang, W., Holbrook, E. H., Lin, B., Herrick, D. B., Peterson, J. N., & Hewitt Coleman, J. (2017). Stem and progenitor cells of the mammalian olfactory epithelium: Taking poietic license. *The Journal of Comparative Neurology*, *525*(4), 1034–1054. http://doi.org/10.1002/cne.24105

Shah, A. N., Davey, C. F., Whitebirch, A. C., Miller, A. C., & Moens, C. B. (2015). Rapid reverse genetic screening using CRISPR in zebrafish. *Nature Methods*, *12*(6), 535–40. http://doi.org/10.1038/nmeth.3360

Shang, J., Cafaro, J., Nehmer, R., & Stone, J. (2010). Supporting Cell Division Is Not Required for Regeneration of Auditory Hair Cells After Ototoxic Injury In Vitro. *Journal of the Association for Research in Otolaryngology*, *11*(2), 203–222. http://doi.org/10.1007/s10162-009-0206-7

Slowik, A. D., & Bermingham-McDonogh, O. (2013). Hair cell generation by notch inhibition in the adult mammalian cristae. *Journal of the Association for Research in Otolaryngology : JARO*, *14*(6), 813–28. http://doi.org/10.1007/s10162-013-0414-z

Sobkowicz, H. M., August, B. K., & Slapnick, S. M. (1997). Cellular interactions as a response to injury in the organ of Corti in culture. *International Journal of Developmental Neuroscience : The Official Journal of the International Society for Developmental*

Neuroscience, *15*(4–5), 463–85. Retrieved from http://www.ncbi.nlm.nih.gov/pubmed/9263026

Steiner, A. B., Kim, T., Cabot, V., & Hudspeth, a J. (2014). Dynamic gene expression by putative hair-cell progenitors during regeneration in the zebrafish lateral line. *Proceedings of the National Academy of Sciences of the United States of America*, *111*(14), E1393-401. http://doi.org/10.1073/pnas.1318692111

Suli, A., Watson, G. M., Rubel, E. W., & Raible, D. W. (2012). Rheotaxis in larval zebrafish is mediated by lateral line mechanosensory hair cells. *PloS One*, *7*(2), e29727. http://doi.org/10.1371/journal.pone.0029727

Tabor, K. M., Bergeron, S. A., Horstick, E. J., Jordan, D. C., Aho, V., Porkka-Heiskanen, T., … Burgess, H. A. (2014). Direct activation of the Mauthner cell by electric field pulses drives ultrarapid escape responses. *Journal of Neurophysiology*, *112*(4), 834–44. http://doi.org/10.1152/jn.00228.2014

Taylor, G., Lehrer, M. S., Jensen, P. J., Sun, T. T., & Lavker, R. M. (2000). Involvement of follicular stem cells in forming not only the follicle but also the epidermis. *Cell*, *102*(4), 451–61. Retrieved from http://www.ncbi.nlm.nih.gov/pubmed/10966107

Thomas, E. D., Cruz, I. A., Hailey, D. W., & Raible, D. W. (2015). There and back again: development and regeneration of the zebrafish lateral line system. *Wiley Interdisciplinary Reviews: Developmental Biology*, *4*(1), 1–16. http://doi.org/10.1002/wdev.160

Tucci, D. L., & Rubel, E. W. (1990). Physiologic Status of Regenerated Hair Cells in the Avian Inner Ear following Aminoglycoside Ototoxicity. *Otolaryngology-Head and Neck Surgery*, *103*(3), 443–450. http://doi.org/10.1177/019459989010300317

Vanwalleghem, G., Heap, L. A., & Scott, E. K. (2017). A profile of auditory-responsive neurons in the larval zebrafish brain. *Journal of Comparative Neurology*, *525*(14), 3031–3043. http://doi.org/10.1002/cne.24258

Viader-Llargués, O., Lupperger, V., Pola-Morell, L., Marr, C., & López-Schier, H. (2018). Live cell-lineage tracing and machine learning reveal patterns of organ regeneration. *ELife*, *7*. http://doi.org/10.7554/eLife.30823

Wada, H., Dambly-Chaudière, C., Kawakami, K., & Ghysen, A. (2013). Innervation is required for sense organ development in the lateral line system of adult zebrafish. *Proceedings of the National Academy of Sciences of the United States of America*, *110*(14), 5659–64. http://doi.org/10.1073/pnas.1214004110

Wada, H., Ghysen, A., Asakawa, K., Abe, G., Ishitani, T., & Kawakami, K. (2013). Wnt/Dkk Negative Feedback Regulates Sensory Organ Size in Zebrafish. *Current Biology*, *23*(16), 1559–1565. http://doi.org/10.1016/J.CUB.2013.06.035

Warchol, M. E., Lambert, P. R., Goldstein, B. J., Forge, A., & Corwin, J. T. (1993). Regenerative proliferation in inner ear sensory epithelia from adult guinea pigs and humans. *Science (New York, N.Y.)*, *259*(5101), 1619–22. Retrieved from http://www.ncbi.nlm.nih.gov/pubmed/8456285

White, P. M., Doetzlhofer, A., Lee, Y. S., Groves, A. K., & Segil, N. (2006). Mammalian

cochlear supporting cells can divide and trans-differentiate into hair cells. *Nature*, *441*(7096), 984–987. http://doi.org/10.1038/nature04849

Wibowo, I., Pinto-Teixeira, F., Satou, C., Higashijima, S., & López-Schier, H. (2011). Compartmentalized Notch signaling sustains epithelial mirror symmetry. *Development (Cambridge, England)*, *138*(6), 1143–1152. http://doi.org/10.1242/dev.060566

Wiedenmann, J., Ivanchenko, S., Oswald, F., Schmitt, F., Rocker, C., Salih, A., … Nienhaus, G. U. (2004). EosFP, a fluorescent marker protein with UV-inducible green-to-red fluorescence conversion. *Proceedings of the National Academy of Sciences*, *101*(45), 15905–15910. http://doi.org/10.1073/pnas.0403668101

Williams, J. a., & Holder, N. (2000). Cell turnover in neuromasts of zebrafish larvae. *Hearing Research*, *143*(1–2), 171–181. http://doi.org/10.1016/S0378-5955(00)00039-3

Xiao, T., Roeser, T., Staub, W., Baier, H., Nüsslein-Volhard, C., & Bonhoeffer, F. (2005). A GFP-based genetic screen reveals mutations that disrupt the architecture of the zebrafish retinotectal projection. *Development (Cambridge, England)*, *132*(13), 2955–67. http://doi.org/10.1242/dev.01861

Yamamoto, N., Tanigaki, K., Tsuji, M., Yabe, D., Ito, J., & Honjo, T. (2006). Inhibition of Notch/RBP-J signaling induces hair cell formation in neonate mouse cochleas. *Journal of Molecular Medicine*, *84*(1), 37–45. http://doi.org/10.1007/s00109-005-0706-9

Yousefi, M., Li, L., & Lengner, C. J. (2017). Hierarchy and Plasticity in the Intestinal Stem Cell Compartment. *Trends in Cell Biology*, *27*(10), 753–764. http://doi.org/10.1016/j.tcb.2017.06.006

Zhang, Q., Li, S., Wong, H.-T. C., He, X. J., Beirl, A., Petralia, R. S., … Kindt, K. S. (2018). Synaptically silent sensory hair cells in zebrafish are recruited after damage. *Nature Communications*, *9*(1), 1388. http://doi.org/10.1038/s41467-018-03806-8